energies

MDPI

Article

Transmission Expansion Investment Evaluation Considering the Impact of Behind-the-Meter Generation

Juan Pablo Rincón Ochoa [1], Alejandro José Salas [1], Mario Alberto Rios [1], Alejandra Tabares [2], Sergio Cabrales [2] and Paulo M. De Oliveira-De Jesus [1,*]

[1] Department of Electrical and Electronic Engineering, School of Engineering, Universidad de Los Andes, Bogotá 111711, Colombia; j.rincono@uniandes.edu.co (J.P.R.O.); a.salasd@uniandes.edu.co (A.J.S.); mrios@uniandes.edu.co (M.A.R.)
[2] Department of Industrial Engineering, School of Engineering, Universidad de Los Andes, Bogotá 111711, Colombia; a.tabaresp@uniandes.edu.co (A.T.); s-cabral@uniandes.edu.co (S.C.)
* Correspondence: pm.deoliveiradejes@uniandes.edu.co

Abstract

Behind-the-meter (BTM) generation is growing rapidly worldwide. Peak demand can be significantly reduced through the increasing installation of rooftop photovoltaic (PV) systems and battery energy storage systems (BESSs). The rate of this reduction is expected to increase with the quality of the solar resource. Transmission expansion plans can therefore benefit from avoided and deferred investment, which must be properly evaluated. These savings, from infrastructure no longer needed, can be passed on to end users through lower network tariffs. This article presents a new methodology for valuing the transmission investment deferred or avoided by BTM generation. BTM generation is represented as a nodal reduction in annual peak demand in static and multi-period DC mixed-integer linear expansion models, and a BTM Index (BTMI) ranks the nodes (substations) where BTM deployment should be promoted. Applied to the Garver system and the Colombian 500 kV backbone, the methodology shows that the required transmission investment decreases as BTM penetration grows, and that part of it is postponed: in Colombia, a 5% penetration removes 30% of the base plan, and final penetrations of 10% and 20% reduce its present value by 27.5% and 53.7%, respectively.

Keywords: transmission expansion planning; behind-the-meter generation; deferred investment credit; net demand; mixed-integer linear programming; behind-the-meter index

Check for updates

Academic Editor: Pavlos S. Georgilakis

Received: 2 November 2026
Revised: 19 November 2026
Accepted: 21 November 2026
Published: 25 November 2026

Copyright: © 2026 by the authors. Licensee MDPI, Basel, Switzerland. This article is an open access article distributed under the terms and conditions of the Creative Commons Attribution (CC BY) license.

1. Introduction

Transmission expansion planning (TEP) decides which circuits to build, and when, so that the network can carry the annual peak power demand projected over a long time horizon [1,2]. That expected demand enters the problem as a fixed input.

The premise is losing ground as behind-the-meter (BTM) generation and storage spread: when users cover part of their own consumption, for instance, by installing rooftop photovoltaic systems with batteries or by acting as small low-voltage distributed generators, the demand to serve at the transmission level is smaller than the gross peak demand projection, and if the reduction happens at given high-voltage substations or nodes it can postpone the investment in a new corridor, shifting or removing it from the plan.

This change is already visible in the data. Table 1 summarizes the penetration of BTM generation in eight systems with recent statistics. Penetration is measured as the share of gross energy demand, the demand that would reach the grid without BTM generation,

that is covered behind the meter. It ranges from about 1% in Colombia to almost 14% in Australia, and reaches 5% or more in four of the eight systems.

Spain illustrates how fast this share can grow. Figure 1 shows the electricity supplied in Spain between 2018 and 2025, separating centralized generation from behind-the-meter generation [3]. BTM generation was negligible until 2021, reached about 4.3 TWh in 2022 and 13.5 TWh in 2025, about 5% of the total supply.

Over the same period centralized generation remained below its 2018 level, and between 2022 and 2025 behind-the-meter generation accounted for about 60% of the increase in total supply. The effect on the network is larger than the energy share suggests, because this generation is concentrated in a few hours of the day.

Table 1. Penetration of behind-the-meter (BTM) generation in selected systems. Gross energy demand includes the BTM energy generation; net energy demand is the energy demand served by the grid; the BTM share is given with respect to gross demand. SG: self-generation; DG: small-scale distributed generation, including exports; PV: BTM solar generation.

System	Year	Gross Demand (TWh)	Net Demand (TWh)	BTM (TWh)	BTM Share (%)	Ref.
Australia	2025	244.5	210.5	33.9	13.9 (DG)	[4]
California	2025	303.0	272.7	30.3	10.0 (PV)	[5]
Brazil	2025	775.9	721.4	54.5	7.0 (DG)	[6]
Spain	2025	269.6	256.1	13.5	5.0 (SG)	[3]
Germany	2025	482.9	466.0	16.9	3.5 (SG)	[7]
Italy	2024	312.3	301.6	10.7	3.4 (SG)	[8,9]
Portugal	2024	54.3	52.8	1.5	2.7 (SG)	[10]
Colombia	2025	85.3	84.4	0.9	1.1 (DG) *	[11,12]

* Estimate from the UPME demand projections; installed capacity of 587 MW of small-scale self-generation and 74 MW of distributed generation at the end of 2025.

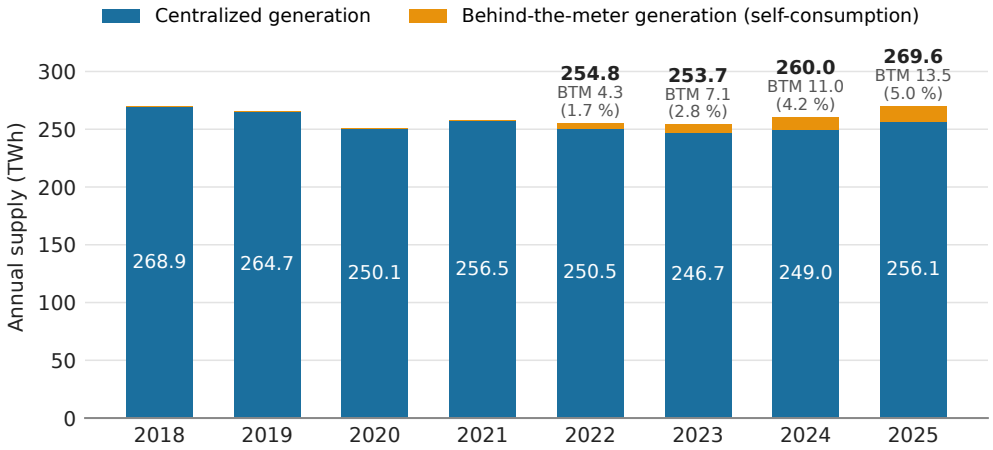


Figure 1. Annual electricity supplied in Spain, 2018–2025: centralized generation and generation behind the meter (distributed generation and self-generation), in TWh. Labels above the bars give the total supply and the behind-the-meter contribution with its share of the total. Data: OMIE [3].

Transmission planning has not kept pace with this change. Table 2 reviews the current long-term transmission expansion plans of the same eight systems and asks two questions: whether the annual peak power demand forecast, typically reached at night, used by the plan accounts for the peak power demand displaced by BTM generation (PV and BESSs), and whether that effect is represented at the nodal level, that is, allocated to the substations where it occurs. Most plans now recognize BTM generation in some form, but only Germany, and California through its demand forecast, represent its effect at the substations of the

network model. The other plans either work with system-wide or zonal aggregates or do not discount the BTM generation from the demand at all.

Table 2. Treatment of BTM generation in current long-term transmission expansion plans.

System	Plan	Horizon	BTM Displacement or Reduction in the Peak Demand	Nodal BTM Effect	Remark
Australia	AEMO, 2026 Integrated System Plan [13]	2026–2050	Explicit	Partial: subregional in the plan; connection-point forecasts published separately	Consumer resources are central: 87 GW of small-scale solar and 35 GW of home batteries by 2050
California	CAISO, 2025–2026 Transmission Plan [14]	2026–2035	Explicit, through the CEC forecast	Yes: CEC bus-level allocation; BTM PV modeled at each bus, BTM storage netted from the bus load	More than half of the USD 6.7 billion plan is driven by load growth
Brazil	EPE, Ten-Year Energy Expansion Plan 2035 [15]	2026–2035	Explicit	No: system and state aggregates	Distributed generation already covers up to 40% of the load at some hours and reverses flows at transmission substations
Spain	MITECO, Transmission Grid Plan 2021–2026 [16]; 2025–2030 proposal [17]	2021–2026	Recognized, not discounted	No	Demand projected as total consumption; the new proposal targets industrial and hydrogen access requests
Germany	TSOs/BNetzA, Grid Development Plan 2037/2045 [18]	2037, 2045	Explicit	Yes: rooftop PV and home batteries assigned to substations	Models prosumer behavior and batteries operated to reduce residual-load peaks
Italy	Terna, Development Plan 2025 [19]	2025–2034	Implicit, through the residual load	Partial: zonal	Recognizes the prosumer model and reverse flows
Portugal	REN, PDIRT-E 2024 [20]	2025–2034	Not explicit	Not identified	Driven by electrification and large new loads
Colombia	UPME, Transmission Expansion Plan 2025–2039 [21]	2025–2039	Partial: one demand scenario	No: national aggregate	Distributed generation enters only as a national reduction of about 0.9 TWh in 2025

The two systems, Germany and California, that represent the effect at the nodal level follow a similar procedure. In Germany, the scenario framework of the grid development plan projects rooftop PV and home storage, assigns the installed capacity by the geographic location of the installations, maps it to the grid topology and the corresponding substations, and simulates the operation of prosumer households, including batteries dispatched to reduce residual-load peaks [18]. In California, the transmission planning process takes the peak demand forecast of the California Energy Commission together with its allocation to the buses of the network model. BTM PV is represented explicitly at each bus through composite load models, with an output adjusted to the hour of each study case, while BTM storage, for which granular location data are lacking, is netted from the load of the corresponding buses; energy efficiency and other load modifiers are also applied bus by bus [5,22,23]. In both cases, the planner sees where the peak demand reduction occurs and when.

The remaining plans miss part of this information, which is the main weakness of a planning approach that ignores BTM generation. A forecast that does not discount BTM generation overstates the demand that the network has to carry and leads to circuits that may be underused; a forecast that discounts it only as a system-wide aggregate cannot tell which corridors are relieved, and therefore cannot tell which investments can be avoided or postponed; and neither of them anticipates the reverse flows that appear when local generation exceeds local demand, as already observed at transmission substations in Brazil [15]. Spain is an example. The current Spanish plan, the Development Plan for the Electricity

Transmission Grid 2021–2026, approved in March 2022 [16], explicitly considered BTM generation and electric vehicles. BTM generation was considered conservatively and without discounting demand: since the national energy and climate plan in force at the time did not include a self-generation target [16], the projected energy demand corresponded to total consumption, without subtracting the energy self-generated in space and time. The plan therefore recognized BTM generation as distributed generation and as a potential factor of net demand reduction, but did not incorporate a quantified assumption on the displacement of grid consumption by dispersed and self-generation [24].

In Colombia, transmission expansion planning takes as its basic input the long-term trend growth of energy and peak power demand in the National Interconnected System, which depends on variables such as gross domestic product, population and energy prices [11]. A demand study suited to the current transition should, however, treat three effects separately: concentrated loads, such as electric mass transit and data centers connected to the main grid; private electric vehicles; and the reduction in demand by generation behind the meter. In general form, for node or substation i,

$$d_i^{\text{net}} = d_i^{\text{trend}} + l_i^{\text{conc}} + d_i^{\text{EV}} - g_i^{\text{BTM}}, \tag{1}$$

where d_i^{trend} is the trend demand, l_i^{conc} is the concentrated loads, d_i^{EV} is the demand of electric vehicles and g_i^{BTM} is the BTM generation considering small-sized low-voltage distributed generation and self-generation at residential, commercial and industrial sectors, including large artificial intelligence data centers with their own generation.

In the current Colombian practice, the spatial estimate of g_i^{BTM} is not an input to transmission planning: distributed generation and self-generation enter the demand projections only as a national scenario [11]. This paper addresses precisely that term, and asks how much transmission investment it can avoid or postpone when it is represented node by node.

To address this gap, this paper proposes a new methodology to quantify the avoided and deferred transmission investment costs. The question it addresses is whether, and by how much, the capital expenditure required by the transmission network falls as BTM penetration grows at each node (substation) of the transmission network, in a system where new demand is supplied behind the meter rather than connected directly to the grid. The resulting savings can be transferred as credits to end users.

The paper makes four contributions. First, a static mixed-integer linear expansion model with a DC network representation (MILP-DC) in which nodal demand enters as $d_i(1 - \alpha_i)$, so that BTM penetration becomes an explicit planning input and the avoided investment is read directly from the optimal plan. Second, a multi-period extension with per-period construction decisions and a present-value objective, which separates investment that is avoided from investment that is only postponed. Third, a BTM Index (BTMI) that captures the potential of BTM penetration at each node or transmission substation, through individual self-generation or energy communities, combines solar potential, nodal supply deficit and the loading of adjacent corridors, and guides deployment toward the nodes where the deferral or avoided cost credit per unit of penetration is largest. This credit can be passed on to end users through lower network tariffs. Fourth, the application of the methodology to two cases: the classical six-bus Garver system, where the mechanism can be followed circuit by circuit, and the 500 kV backbone of the Colombian system, as an example of a real network with significant BTM potential.

The rest of the paper is organized as follows. Section 2 reviews the related work, Section 3 presents the conceptual framework, Section 4 the models and the index, Section 5 presents the two case studies, Section 6 presents the results and Section 7 presents the conclusions.

2. Related Work

The TEP literature has refined the network model and the solution methods, from the transportation and hybrid formulations to the full DC model with disjunctive constraints [2], bi-level formulations for market environments [25] and reliability-constrained variants [26,27]. In all of them, demand is exogenous, and any resource other than the line is a supply-side or control element operated by the planner.

A large body of recent work extends TEP to the uncertainty introduced by renewable generation, storage and demand growth. Kim et al. [28] treat peak-demand uncertainty through Monte Carlo simulation and sample average approximation in a multi-stage model tested on the Garver system; Giannelos et al. [29] apply multistage stochastic optimization to the Indian transmission network up to 2060 and show the option value of storage as an alternative to line reinforcement; and Khastieva et al. [30] study the joint planning of transmission and storage and the use of storage to defer line investment. A recent review in this journal classifies the methods for planning with renewables into deterministic, stochastic, robust and AI-enhanced approaches [31]. These works improve how the planner represents variable supply, and they are complementary to the present paper: the resources they consider are connected to the grid and represented as injections or as assets chosen by the planner. This paper does not propose a new TEP model with renewables; it deliberately uses the classical deterministic formulation of Garver and Villasana [1,2] to isolate the effect of BTM on the expansion plan, and any of these stochastic methods can replace it in future work.

The idea that distributed generation can defer network investment has been widely treated in the literature, mainly at the distribution level. Lee et al. [32] examined how dispersed storage and generation change network requirements, and Shugar [33] evaluated the distributed benefits of photovoltaic plants connected to a distribution feeder. The concept was later formalized in several directions. Li and Zielke [34] valued small load reductions through the one-year deferral method; De Oliveira-De Jesus et al. proposed a general framework for remunerating the costs and benefits of distributed generation [35,36], and Mendez et al. [37] assessed deferral under uncertainty through Monte Carlo simulation.

At the transmission level, Luo et al. [38] quantified how distributed generation connected to the network reduces the transmission expansion cost of the Queensland system, with a benefit that depends on location, topology and technical constraints, and a recent 20-year study of the Western United States found that faster adoption of distributed generation could delay or avoid some transmission upgrades, although some expansion remains necessary in every case [39]. The latter works with system-wide adoption scenarios and does not represent the effect node by node or compute a present-value deferral/avoided credit.

Recent work on non-wires alternatives (NWAs) values distributed energy resources as substitutes for network upgrades. Laws et al. [40] formulate a bilevel problem that compares utility-owned batteries, conventional upgrades and energy purchased from private DER owners, and derive a time- and location-specific price signal for those owners; a review of utility practice [41] finds that DER-based deferral has had limited uptake, in part because these alternatives are seldom suitable for serving new connections, consistent with the floor found in this paper; and Carvallo et al. [42] measure the technical, economic and rate impacts of distributed solar, electric vehicles and storage, the components of the net demand.

Previous studies remain at the distribution level or at the scale of bulk generation; none of them re-optimizes a transmission expansion plan under a nodal BTM penetration. A parallel line values the contribution of renewables and storage to generation adequacy, the capacity credit [43], which Liu et al. [44] extended to multi-area systems where transfer limits make the credit location-dependent.

Most of these works credit a resource for what it injects. Whether it is a distributed generator, a central renewable plant or a storage unit, it is connected to the grid, it appears in the nodal balance as an injection, and its benefit is measured against that injection. BTM generation does not fit that description: it never reaches the network, it is not dispatched by the operator, and its only trace in the planning problem is a smaller withdrawal at the node. The closest antecedent is the one-year deferral method of Li and Zielke [34], which explicitly values reductions in the forecast peak demand: in their transformer example, a load reduction postpones the expansion by one year. The method is marginal and ex post: it takes the expansion plan as fixed, does not represent the network and values small reductions by shifting a planned project in time. This approach is appropriate for the small reductions it was designed for. At the penetrations now enabled by PV with storage (Table 1), however, a demand reduction can change the topology of the optimal plan, not only the timing of a fixed project, which requires re-optimizing the plan with an explicit network representation. Table 3 lists these contributions side by side.

Table 3. State of the art. Level: Tx transmission, Dx distribution, Gen generation adequacy, EC energy community. Credit: network, avoided or deferred network investment; capacity, contribution to adequacy.

Reference	Year	Level	Resource	Credit?	Multi-Period?	Siting Priority?
[38]	2014	Tx	DG	yes	no	no
[28]	2018	Tx	none (uncertainty)	no	yes	no
[30]	2019	Tx	BESS	yes	no	no
[39]	2024	Tx	DG	yes	yes	no
[32]	1979	Tx	DG	yes	no	no
[33]	1990	Dx	DG	yes	no	no
[37]	2003	Dx	DG	yes	no	no
[34]	2005	Tx, Dx	load reduction	yes	no	no
[35]	2006	Dx	DG	yes	no	no
[42]	2021	Dx	DG and EV	no	yes	no
[41]	2022	Dx	NWA	yes	no	no
[40]	2024	Dx	NWA	yes	no	yes
[44]	2021	Gen	DG and BESS	yes	no	partial
This paper	2026	Tx	BTM	yes	yes	yes

The last row of Table 3 makes the gap explicit: no previous work combines the deferral credit, the multi-period evaluation and the siting priority of the BTM resource, that is, the nodal reduction due to PV and BESSs, in the same methodological approach. Previous studies either credit resources that inject into the grid [35,38], value marginal load reductions against a fixed plan [34], or assess distributed solar through system-wide adoption scenarios [39]. To the best of our knowledge, this is the first work that applies the deferred transmission investment credit to behind-the-meter generation, such as rooftop PV with storage, represented as a nodal reduction in net demand within a transmission expansion model where the TEP is re-optimized for each BTM penetration level.

3. Conceptual Framework

This section presents the conceptual framework of this proposal.

3.1. The Behind-the-Meter Resource as a Reduction in Peak Power Demand

A transmission corridor is sized to carry the difference between the power generated and the power consumed on each side of it at peak time. Any resource that reduces consumption at the importing end therefore has the same effect on the corridor as an increase in its capacity, without a single kilometer of conductor being installed. In this

sense, BTM generation can be interpreted as a virtual transmission asset: it does not inject power into the backbone, and it is not dispatched by the system operator, but it does change the quantity the backbone has to transport (Figure 2).

Formally, let d_i be the nodal peak active power demand projected at node or transmission substation i, which typically occurs at night, before the BTM discount. The peak power demand seen by the transmission system at each node i is defined as:

$$d_i^{\text{net}} = d_i\,(1 - \alpha_i) \tag{2}$$

where $\alpha_i \in [0, 1]$ is a penetration factor defined as the fraction of that peak demand served locally by generation and storage operated behind the meter. If the peak occurs at night, the α_i factor incorporates BESS power injections of PV energy stored during solar hours and/or self-generation associated with other sources such as wind, biofuels or co-generation.

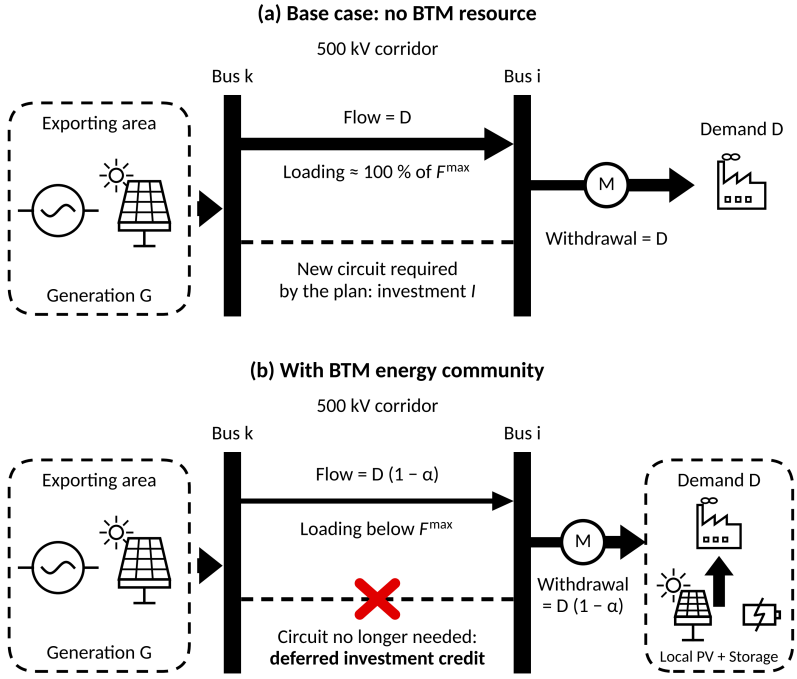


Figure 2. Behind-the-meter self-generation interpreted as a virtual transmission asset: BTM generation reduces the net demand carried by the backbone and relieves the adjacent corridors.

Equation (2) is the compact form of Equation (1): $d_i = d_i^{\text{trend}} + l_i^{\text{conc}} + d_i^{\text{EV}}$ is the nodal peak power demand before the BTM discount, and the penetration is the BTM generation available at the peak hour expressed as a fraction of that demand, $\alpha_i = g_i^{\text{BTM}}/d_i$. The nodal gross peak active power demand d_i is the reference forecast of the planner at node i. Its three terms are projected without any discount for BTM generation.

The trend term is estimated from the historical demand measured at the grid, which already reflects the BTM generation installed in the base year, so α_i is the additional BTM generation with respect to that reference and no reduction is counted twice. Accordingly, the savings reported in this paper measure the transmission value of additional BTM generation relative to a reference scenario without it. They are not a benefit of the method over planning based on net demand, since a planner who already used the same net demand would obtain the same plan; the contribution of the method is to measure that value, attribute it to the BTM resource and locate it in the network.

Equation (2) is algebraically equivalent to a fixed, cost-free active power injection $\alpha_i d_i$ in the nodal power balance, and the optimal plans would be identical under either

representation. The distinction is therefore not mathematical; it concerns who decides on the resource and how it enters the planning process.

First, BTM resources are not dispatched by a central authority but self-dispatched by each prosumer according to an individual benefit function, in response to day-ahead price signals [45]. In the model, α_i is an exogenous parameter rather than a decision variable, so the planner cannot re-dispatch or curtail it, whereas the central generation g_i is chosen by the optimizer. Second, connection: the resource does not export to the transmission network and requires no connection capacity in it; since $\alpha_i \in [0, 1]$, the net demand never becomes negative and the node at the transmission level never exports. Third, information: in planning practice, BTM generation enters through the demand forecast, not through the generation expansion plan, as in the German and Californian plans of Table 2; representing it as a reduction in net demand reproduces that practice. Resource availability is addressed by interpreting the penetration factor as a firm supply at the peak hour, and the requirement of backup supply is discussed in Section 6.4.

The BTM penetration factor α_i aggregates every form of generation behind the point of connection at node i: individual self-generation of any size, collective schemes in which several users share a single metering boundary and energy communities in general [46,47]. From the point of view of the backbone the legal or commercial arrangement is irrelevant, because all of them produce the same effect, a smaller net withdrawal at the node. The same holds for a large load that connects with its own generation behind the meter: its consumption is served locally and does not reach the transmission network.

Market evidence points to stronger BTM generation based on PV and BESS technologies since levelized costs of electricity of solar systems with storage are increasingly competitive [48]. Daytime wholesale prices have collapsed where solar penetration is high: Spain recorded almost 800 h of zero or negative day-ahead prices by October 2024 [49], and since February 2025, new PV systems in Germany receive no feed-in remuneration during negative-price hours [50]. PV that only exports at midday therefore loses value, and self-generators and distributed generators add storage to cover their evening demand and sell surpluses at higher evening prices, an arbitrage that can be built into the optimal sizing of PV and storage [45]. In California, the share of new residential PV systems paired with storage rose from about 10% to about 60% after the 2023 net billing tariff [51].

Where PV with storage is the dominant BTM technology, as in the systems of Table 1, the premise of this paper is that α_i will be larger at nodes with higher solar irradiation, because more hours of resource make the storage that enables night-time supply more viable. The spatial deployment of BTM generation is thus expected to correlate positively with the historical mean irradiation. This is a working hypothesis: irradiation is a necessary condition for PV with storage, not the only driver of its deployment.

3.2. Avoided and Deferred Transmission Investment Due to BTM Peak Demand Reduction

The benefit that a given BTM penetration produces is not the same quantity in a single-horizon study and in a study that follows the system year by year, and the two are often confused. A static model compares the optimal plan for a target year with and without BTM resources. The difference is investment that the plan no longer contains, that is, avoided investment:

$$C^{\mathrm{av}}(\alpha) = I^{\mathrm{base}} - I(\alpha) \tag{3}$$

where the penetration vector is $\alpha = [\alpha_1, \ldots, \alpha_i, \ldots, \alpha_n]$, with n being the number of nodes, I^{base} being the cost of the optimal plan with $\alpha_i = 0$ for all nodes (the base-case TEP plan without BTM effect) and $I(\alpha)$ being the cost of the optimal plan under the BTM penetration vector α, with a different α_i at each node i. The average value of the penetration vector α is denoted as $\bar{\alpha}$.

Under a multi-period TEP model, we decide not only which circuits to build but also in which year. Under a penetration that grows over time, a circuit that the base plan requires early may be pushed toward the end of the horizon, or out of it. Because the planner discounts, a circuit built later is worth less today, and the benefit is measured as a difference of present values:

$$C^{\text{def}}(\alpha) = \sum_{t \in T} \frac{I_t^{\text{base}}}{(1+r)^{t-1}} - \sum_{t \in T} \frac{I_t(\alpha)}{(1+r)^{t-1}} \tag{4}$$

with r being the discount rate and I_t being the investment committed in period t. Equation (4) captures both effects at once: a circuit that disappears from the plan contributes its full cost, and a circuit that is merely delayed contributes the financial value of the delay, in the spirit of the one-year deferral method [34]. Throughout the paper, deferred credit refers to Equation (4) and avoided investment to Equation (3).

The connection of large data centers directly to the transmission system should not affect the avoided cost or the deferred credit, since the specific reinforcements they require are funded by their developers.

3.3. Where to Deploy: Uniform and Prioritized Allocation

Since the effect of a reduction depends on the location of node (substation) i, a total penetration budget can be distributed in different ways. Two allocations are compared.

First, the uniform allocation assigns the same fraction everywhere, $\alpha_i = \bar{\alpha}$, and represents a policy that is blind to the state of the network.

Second, the prioritized allocation distributes the same aggregate penetration in proportion to a composite index,

$$\alpha_i = \min\left(\bar{\alpha} \frac{BTMI_i}{\overline{BTMI}},\ \alpha^{\max} \right) \tag{5}$$

where $BTMI_i$ is the BTM Index of node i, $\overline{BTMI}$ is its mean over the nodes with demand and $\alpha^{\max}$ is a cap that prevents any single node from being assigned an implausible penetration.

The BTM Index combines what makes a node attractive for BTM generation, individual or collective, and what makes it valuable for the grid: the solar resource available at its location, the gap between local generation and local demand and how loaded the corridors around it already are.

Its formal definition is given in Section 4. Comparing the two allocations at equal aggregate penetration isolates the value of siting, separately from the value of the resource itself.

4. Methodology

The proposed method has two stages, shown in Figure 3. In the first stage, the state of the network in the target year, together with the solar resource, produces the index and the two penetration vectors. In the second stage, the transmission expansion models are solved, first with no BTM resources to obtain the base plan and then for each penetration level and each allocation strategy. The static model returns the avoided investment and the multi-period model returns the construction schedule and the deferred credit. Nothing in the second stage feeds back into the first: the index is computed from the base case, so the prioritization does not depend on the plan it helps to modify.

In the following, we define the general assumptions of the method, the TEP models (static and multi-period), the BTM allocation strategies based on the BTMI and the general algorithm. The notation is summarized in the Nomenclature at the end of the paper. Real power quantities are handled in per unit in the models and reported in MW in the text and tables.

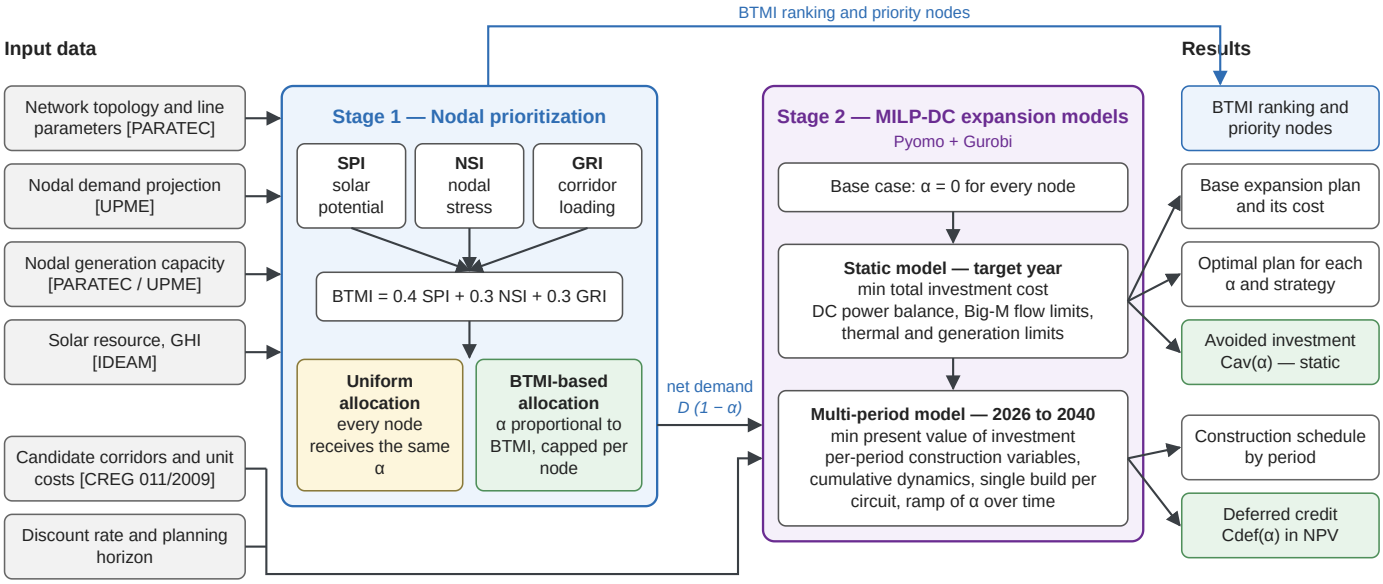


Figure 3. General framework: construction of the BTM Index and evaluation of the static and multi-period expansion plans under each penetration level.

4.1. Assumptions

The models share a set of assumptions that define the scope of the analysis. The network is represented by a lossless DC power flow, which is standard in expansion planning because the decision of interest is the discrete choice of circuits rather than the operating point. Only the 500 kV level is modeled, so reinforcements at lower voltages and transformation capacity are outside the scope. Circuits are limited by their thermal rating and no security criterion is imposed, which means the plans reported here are the minimum set of circuits needed under normal operation. Generation is bounded by the capacity available at each node and is dispatched without cost, so the optimizer selects the dispatch that best relieves the network among all feasible ones. Finally, the penetration vector α is an exogenous, known planning input rather than a decision variable: the models answer what the network would require under a given level of BTM generation.

4.2. Static MILP-DC Model

Let $\mathcal{I}$ be the set of nodes, $\mathcal{J}$ be the set of corridors and $\mathcal{K} = \{1, \ldots, K\}$ be the set of circuit positions available in each corridor, of which the first n_j^0 are already in service. The binary variable $y_{j,k}$ takes the value one when circuit k of corridor j is in service, $f_{j,k}$ is the power flow through it, g_i is the power injected at node i and θ_i is the voltage angle. The problem minimizes the cost of the circuits that have to be built:

$$\min \sum_{j \in \mathcal{J}} \sum_{k \in \mathcal{K},\, k > n_j^0} c_j \, y_{j,k} \tag{6}$$

subject to the nodal power balance, written with the net demand of Equation (2),

$$\sum_{j \in \mathcal{J}} \sum_{k \in \mathcal{K}} S_{ij} f_{j,k} + g_i = d_i \, (1 - \alpha_i), \qquad \forall i \in \mathcal{I} \tag{7}$$

where S_{ij} is the node-corridor incidence, equal to $+1$ if i is the sending end of j, -1 if it is the receiving end and zero otherwise. The DC flow through a circuit is imposed only when that circuit exists, which is written with a disjunctive Big-M formulation:

$$-M_j\,(1-y_{j,k}) \;\le\; f_{j,k} - B_j\,(\theta_a-\theta_b) \;\le\; M_j\,(1-y_{j,k}), \qquad \forall j\in\mathcal{J},\ \forall k\in\mathcal{K} \tag{8}$$

with a and b the ends of corridor j and B_j its susceptance. When $y_{j,k}=1$, the constraint reduces to the DC flow equation, and when $y_{j,k}=0$, it becomes redundant while the thermal limit forces the flow to zero:

$$-F_j^{\max}\,y_{j,k} \;\le\; f_{j,k} \;\le\; F_j^{\max}\,y_{j,k}, \qquad \forall j\in\mathcal{J},\ \forall k\in\mathcal{K} \tag{9}$$

The remaining constraints bound generation, fix the circuits already in service, set the angular reference at the node with the largest net export and cap the total investment when a budget applies:

$$0 \;\le\; g_i \;\le\; G_i^{\max}, \qquad \forall i\in\mathcal{I} \tag{10}$$

$$y_{j,k}=1, \qquad \forall j\in\mathcal{J},\ \forall k\le n_j^0 \tag{11}$$

$$\theta_{\text{ref}}=0 \tag{12}$$

$$\sum_{j\in\mathcal{J}}\sum_{k>n_j^0} c_j\,y_{j,k} \;\le\; \Gamma \tag{13}$$

The parameter M_j deserves a comment, because a value that is too small silently removes feasible plans. Since the left-hand side of Equation (8) is bounded by $B_j\,|\theta_a-\theta_b|$, it is enough to take $M_j = B_j\,\Delta\theta^{\max}$, where $\Delta\theta^{\max}$ bounds the angular difference between any pair of nodes. That bound is computed from the existing network as the largest shortest path between two nodes, weighting each corridor by the angular opening it develops at full load, $X_j F_j^{\max}$, plus twice the opening of the largest candidate corridor to account for the substations that are only reachable through a new circuit.

4.3. Multi-Period MILP-DC Model

The static model answers whether a circuit is needed at a target year. The multi-period model asks when. The horizon is divided into periods $t\in\mathcal{T}=\{1,\dots,T\}$, one per year. The binary variable $y_{j,k,t}$ indicates that circuit k of corridor j is built in period t, and $x_{j,k,t}$ indicates that it is available in that period. The objective is the present value of the investment:

$$\min \sum_{t\in\mathcal{T}}\sum_{j\in\mathcal{J}}\sum_{k>n_j^0} \frac{c_j\,y_{j,k,t}}{(1+r)^{\,t-1}} \tag{14}$$

Equations (7)–(12) are replicated for every period, with $x_{j,k,t}$ in place of $y_{j,k}$ and with demand and generation evaluated at each year. Two constraints link the periods. The first states that a circuit available in t is one that was already available in $t-1$ or was built in t, starting from the circuits already in service:

$$x_{j,k,t} = x_{j,k,t-1} + y_{j,k,t}, \qquad x_{j,k,0} = \begin{cases} 1 & k\le n_j^0 \\ 0 & k>n_j^0 \end{cases} \tag{15}$$

The second prevents a circuit from being built more than once, which also keeps $x_{j,k,t}$ binary without declaring it as such:

$$\sum_{t\in\mathcal{T}} y_{j,k,t} \;\le\; 1, \qquad \forall j\in\mathcal{J},\ \forall k\in\mathcal{K} \tag{16}$$

Demand and generation are interpolated linearly between the anchor years of the projection, and behind-the-meter penetration is introduced as a ramp that starts at zero

in the first period and reaches its final value at the end of the horizon, which represents progressive adoption rather than an installed base:

$$\alpha_{i,t} = \alpha_i \frac{t-1}{T-1}, \qquad \forall i \in \mathcal{I},\ \forall t \in \mathcal{T} \tag{17}$$

The deferred credit of Equation (4) is obtained by solving Equation (14) with $\alpha_i = 0$ and then with the penetration vector under evaluation, and comparing the two present values.

4.4. BTM Index

The BTM Index (BTMI) captures the potential of BTM penetration at each node, whether it comes from individual self-generation or from energy communities. It ranks nodes by how much a reduction in net demand at that node is worth to the transmission system, and by how easily BTM generation could produce that reduction. It combines three normalized sub-indices.

The solar potential index rewards the availability of the resource, using the daily global horizontal irradiation at the node:

$$SPI_i = \frac{GHI_i}{\max_{n \in \mathcal{I}} GHI_n} \tag{18}$$

The nodal stress index measures how much of the local demand is not covered by local generation, so that exporting nodes score zero:

$$NSI_i = \frac{1}{\eta_N} \max\left(0,\ \frac{d_i - G_i^{\max}}{d_i}\right), \qquad \eta_N = \max_{n \in \mathcal{I}} \max\left(0,\ \frac{d_n - G_n^{\max}}{d_n}\right) \tag{19}$$

The grid reinforcement index accumulates the loading of the corridors incident to the node, capped at full load so that a single saturated corridor does not dominate the sum:

$$GRI_i = \frac{1}{\eta_G} \sum_{j \in \Omega_i} \min\left(\frac{|\hat{f}_j|}{\max(n_j^0, 1)\, F_j^{\max}},\ 1\right) \tag{20}$$

where Ω_i is the set of corridors incident to node i, $\hat{f}_j$ is the flow of the base case and η_G is the largest value of the sum over the nodes; the maximum with one prevents a zero capacity for candidate corridors with no circuit in service. The three components are combined with fixed weights:

$$BTMI_i = 0.4\, SPI_i + 0.3\, NSI_i + 0.3\, GRI_i \tag{21}$$

The weights give priority to the resource, because BTM generation, individual or collective, cannot be developed where there is no resource to harvest, and more hours of resource make the storage that provides a firm contribution at the peak hour more viable (Section 3), and split the remainder evenly between the two grid-related terms, which measure the same congestion from the node side and from the corridor side. This weighting follows the practice of multicriteria studies on energy systems [52,53]. The index feeds the allocation rule of Equation (5), and nodes without demand receive no penetration. The cap is set at $\alpha^{max} = 0.40$ for the Colombian backbone; it is not applied to the Garver system, for the reason given in Section 5.1.

4.5. Procedure

The complete procedure is given in Algorithm 1.

Algorithm 1 Deferred transmission investment credit with BTMI-based prioritization.

Require: Network topology and line parameters; nodal demand and generation projections; candidate corridors and unit costs; daily global horizontal irradiation; discount rate r and horizon T

Ensure: Base plan, avoided investment $C^{\mathrm{av}}(\alpha)$, construction schedule and deferred credit $C^{\mathrm{def}}(\alpha)$

1: Assemble the input data and compute B_j, $F_j^{\max}$, c_j and M_j for every corridor
2: Solve the static model Equations (6)–(13) with $\alpha_i = 0$ for the target year
3: Store the base plan, its cost I^{base} and the corridor loadings $\hat{f}_j$
4: Compute SPI_i, NSI_i and GRI_i from the base case using Equations (18)–(20)
5: Obtain $BTMI_i$ from Equation (21) for every node with demand
6: **for** each aggregate penetration level $\bar{\alpha}$ **do**
7: Build the uniform vector $\alpha_i = \bar{\alpha}$ and the BTMI-based vector from Equation (5)
8: **for** each allocation strategy **do**
9: Solve the static model with the net demand $d_i(1 - \alpha_i)$
10: Compute the avoided investment $C^{\mathrm{av}}(\alpha)$ from Equation (3)
11: Solve the multi-period model Equations (14)–(17) with the penetration ramp
12: Compute the deferred credit $C^{\mathrm{def}}(\alpha)$ from Equation (4)
13: Compare both strategies at equal aggregate penetration and identify the corridors that leave the plan at each level

Steps 2 and 10 answer how much investment a given penetration avoids, steps 11 and 12 separate what is avoided from what is only postponed and step 13 isolates the value of siting the resource.

5. Case Study

The models are applied to two systems: the six-bus Garver system, where the mechanism can be observed in isolation, and an equivalent of the 500 kV backbone of the Colombian National Interconnected System.

5.1. Garver Test System

The six-bus system introduced by Garver [1] is the standard benchmark for expansion planning. It has 760 MW of demand and 760 MW of available capacity, distributed as shown in Table 4, and 15 possible corridors, six of which already carry a circuit. Each corridor admits up to five circuits, and the corridor data are given in Appendix A. Bus 6 is isolated in the initial configuration and holds most of the generation, so the plan must connect it: generation far from the load and a network that has to be built to reach it, which is the situation the methodology is meant to address.

Table 4. Demand and generation capacity of the Garver system.

Bus	**1**	**2**	**3**	**4**	**5**	**6**
Demand (MW)	80	240	40	160	240	0
Generation capacity (MW)	50	0	165	0	0	545

The static model is solved for penetrations from 0 to 50% in steps of 10%, the range over which the plan of this system changes. For the multi-period model, demand grows linearly from 55% of the values in Table 4 to their full value over a ten-year horizon, with a discount rate of 10%. In this system, the BTMI allocation is applied without the cap α^{max}. Buses 2, 4 and 5 have almost the same index, so from an aggregate penetration of about 34% the cap would bind at all three importing buses, and at 50%, also at bus 1, and the penetration vector would collapse into a nearly flat 40%, no longer representing the aggregate level

being evaluated. In the Colombian network, the cap binds only at the highest level studied and at a few nodes, so the allocation keeps its spatial differentiation and the cap is retained.

5.2. The Colombian 500 kV Backbone Case Study

Colombia is a useful example because it combines the two conditions the methodology requires. Its backbone links the hydro resources of the Andean region and the wind and solar potential of the Caribbean and La Guajira to load centers several hundred kilometers away, and the reference expansion plan foresees reinforcements on several of those corridors [54]. At the same time, in about a decade, the country has built a regulatory framework that turns BTM generation into a recognized system activity. Resolution CREG 030 of 2018 [55] first regulated small-scale self-generation; Resolution CREG 174 of 2021 [56] consolidated the rules for small-scale (AGPE, below 1 MW) and large-scale (AGGE) self-generation; Law 2099 of 2021 [57] declared non-conventional renewable sources of public utility; Decree 2236 of 2023 [58] and Resolution MME 40509 of 2024 [59] set the legal basis and the registry of energy communities; and Resolution CREG 101 072 of 2025 [60] introduced the collective self-generator and virtual boundary aggregation, with a target of 1 GW from energy communities. In this case study, the penetration factor α_i represents the joint effect of AGPE, AGGE and collective self-generation.

The network is represented by the 21 substations that operate at 500 kV and the 4 substations associated with projects in the reference expansion plan, for a total of 25 nodes. Circuits connecting the same pair of substations are grouped into a corridor, whose susceptance and rating are the average of its circuits; the differences between parallel circuits are below 5% in all cases. This yields 27 existing corridors carrying 31 circuits, and 10 candidate corridors that correspond to planned projects. Line parameters and ratings are taken from the public technical database of the system operator [61]: ratings range from 1650 to 2165 MVA and lengths from 36 to 275 km. As in the Garver case, each corridor admits up to five circuits, so reinforcing an existing corridor is also an option. The corridor data are given in Appendix A.

Investment costs follow the reference construction units of the regulator [62], expressed in December 2008 US dollars. The unit cost of a 500 kV single-circuit line is 259,944 USD/km at the lowest terrain level and 283,990 USD/km at the intermediate level, which gives costs per circuit between USD 10.2M and 78.1M depending on the length of the corridor. The figures reported in Section 6 are therefore not current dollars; since every corridor is costed with the same unit prices, indexing them would scale the whole plan and every saving by the same factor, leaving the comparison between strategies and the relative magnitude of the deferred credit unchanged. The budget constraint Equation (13) is set well above the optimal plan and is never active.

5.3. Nodal Demand and Generation

Demand is projected by the planning unit at the area level [11], and generation capacity is known plant by plant, so both have to be distributed over the nodes. The projection used is the reference gross demand, the sum of the trend demand of the National Interconnected System, the large concentrated loads and electric vehicles, without the distributed generation scenario. The BTM generation installed in the base year, about 1% of the demand (Table 1), is embedded in the historical demand from which the trend is projected, so α_i represents BTM generation penetration. The allocation used here is an approximation, and it is the input that most conditions the results, so the criteria are stated explicitly.

Demand is distributed within each area in proportion to the load each substation actually serves, that is, its transformation capacity toward the lower voltage levels and the urban center it supplies. Substations that are essentially transit or generation nodes receive

little or no demand. Generation is assigned to the substation where each plant connects, and the resulting vector is rescaled so that the national total matches the projection for each anchor year. This is the main difference with respect to an allocation proportional to the connected transmission capacity, which distributes residual generation over transit substations and produces load centers that appear to be self-sufficient. Table 5 shows the resulting allocation.

Table 5. Nodal allocation of demand and generation capacity. Capacity is the installed value assigned to each substation before rescaling to the national total; the 1050 MW of Colectora and a further 1200 MW at Antioquia (completion of Ituango) are added in 2034.

Node	Substation	Area	Area Demand (%)	Capacity (MW)
N3	Bacatá	Oriental	45	1000
N13	Nueva Esperanza	Oriental	45	1213
N16	Primavera	Oriental	10	600
N23	Norte	Oriental	0	0
N11	Medellín	Antioquia	45	120
N8	Heliconia	Antioquia	30	80
N5	Cerromatoso	Antioquia	10	340
N2	Antioquia	Antioquia	10	1200
N15	Porce III	Antioquia	5	1100
N17	Sabanalarga	Caribe	30	1400
N4	Bolívar	Caribe	24	900
N7	El Copey	Caribe	16	400
N12	Nueva Cuestecitas	Caribe	10	400
N6	Chinú	Caribe	8	300
N18	Sahagún	Caribe	7	0
N9	La Loma	Caribe	5	300
N24	Carreto	Caribe	0	0
N25	Nueva Magangué	Caribe	0	0
N22	Colectora	Caribe	0	1050
N21	Sogamoso	Nordeste	65	1000
N14	Ocaña	Nordeste	35	100
N20	San Marcos	Suroccidente	33	300
N1	Alférez	Suroccidente	32	400
N10	La Virginia	Suroccidente	30	600
N19	San Carlos	Suroccidente	5	2200

Three points follow from this allocation. The generation of the Guavio and Chivor complexes reaches the Bogotá area through the 230 kV ring, so it is assigned to the two 500 kV substations of that area, while the Norte substation is left with no generation because the project that would connect it is precisely one of the candidates. The Ituango complex and the Colectora wind hub enter in 2034, which is when their capacity is added at the Antioquia and Colectora nodes. Furthermore, the conditioned demand of the Bogotá savanna, which today cannot be connected because the associated works are not in service, is represented at the Norte node, growing linearly to 400 MW by 2034 and following the scenario ramp thereafter.

Daily solar irradiation is taken from the national solar atlas [63] and assigned by area, at between 4.3 and 4.8 kWh/m^2 per day in the Andean areas and 5.5 kWh/m^2 per day in the Caribbean, with 6.2 kWh/m^2 per day for the two substations located in La Guajira.

5.4. High-Electrification Scenario

The reference projection alone does not stress the backbone enough to make the question meaningful: under that projection, the 2040 plan contains only the USD 24.7M circuit that connects the Norte substation, and no transfer corridor needs reinforcement, although

the most loaded one reaches 93% of its rating. The deferred credit is only meaningful where expansion is needed, so the models are applied to a high-electrification scenario built on top of the reference projection. Demand grows faster in the areas where electrification and urban growth concentrate, and new capacity is added where the resource is, that is, in the Caribbean and La Guajira for wind and solar and, to a lesser extent, in the south-west. The growth factors (G for generation and D for demand) are applied as a ramp, so the initial year keeps the projected values and the factor is reached in full at the end of the horizon. Table 6 reports them.

Table 6. Growth factors of the high-electrification scenario and resulting balance in 2040.

Area	D Factor	G Factor	Demand 2040 (MW)	Capacity 2040 (MW)
Oriental	1.8	1.0	7571	4084
Antioquia	1.5	1.2	3683	7037
Caribe	1.4	2.0	8873	13,790
Nordeste	1.4	1.2	3051	1916
Suroccidente	1.4	1.3	4746	6605
Total			27,925	33,433

The logic of the scenario is transparent: demand grows at the center and capacity grows at the periphery, so the quantity to be transported grows faster than either of them. The system moves from 12,234 MW of demand and 21,271 MW of capacity in 2026 to 27,925 MW and 33,433 MW, respectively, in 2040. The Oriental area, which concentrates the Bogotá load, ends the horizon with a deficit of 3487 MW that has to be imported through the backbone, while the Caribbean ends it with a surplus of 4917 MW.

The multi-period horizon covers 2026 to 2040, one period per year, with a discount rate of 10%. Demand and generation between the anchor years of the projection are interpolated linearly. The angular reference is placed at San Carlos, the node with the largest net export at the target year.

The static model is solved for penetrations from 0 to 30% in steps of 5%; beyond 30%, only the connection of new load remains in the plan.

5.5. Implementation

Both models were written in Pyomo [64] (version 6.1.0) and solved with Gurobi [65] (version 14.0), with an optimality gap of 0.3% for the static model and 0.5% for the multi-period one. The static instance has 185 binary variables, while the multi-period instance has 2775 binary variables, plus 2775 availability variables that remain binary by construction. Both instances are solved within 8 s on a computer HP Notebook 14 DK0022WM equipped with a Ryzen 3 3200U processor with 120 GB SSD and 8 GB of RAM. In the case studies, the multi-period model (step 11 of Algorithm 1) was solved for final penetrations of 10 and 20% under the uniform allocation.

6. Results and Discussion

This section presents the results for the two systems described in Section 5. The six-bus Garver system is used for illustration purposes: it is small enough for the effect of BTM penetration on the optimal plan to be followed circuit by circuit. The equivalent of the Colombian 500 kV backbone is then studied as a real case. In both systems, the case $\alpha = 0$, without BTM generation, corresponds to traditional TEP and is the benchmark for all comparisons.

6.1. Six-Bus Garver Test System Results

Applying the static model to the Garver system with no behind-the-meter resource reproduces the canonical solution of the literature [1]: four circuits on corridor 2–6, one on 3–5 and two on 4–6, seven circuits in total for USD 1000k. The plan coincides, circuit by circuit, with the one reported by Garver [1] and later replicated by Villasana et al. [2] and Vargas-Robayo et al. [27], which verifies the formulation and its implementation before moving to a larger network. The total cost depends on the unit costs adopted, which differ among these references; the values used here are given in Appendix A.

The interest of the test system, however, is that the deferral mechanism can be inspected by hand. Tables 7 and 8 report the optimal investment plans and the avoided costs given by Equation (3) as a function of the BTM penetration under the two allocation strategies.

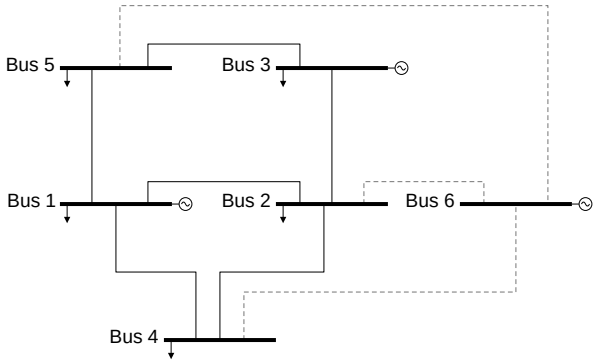
Table 7. Static results on the six-bus Garver system by penetration level: uniform allocation.

$\bar{\alpha}$	d^{net} (MW)	Uniform $I(\alpha)$ (USD 1k)	Avoided Cost $C^{\text{av}}(\alpha)$ (USD 1k)
0%	760	1000	0
10%	684	850	150
20%	608	700	300
30%	532	700	300
40%	456	450	550
50%	380	300	700

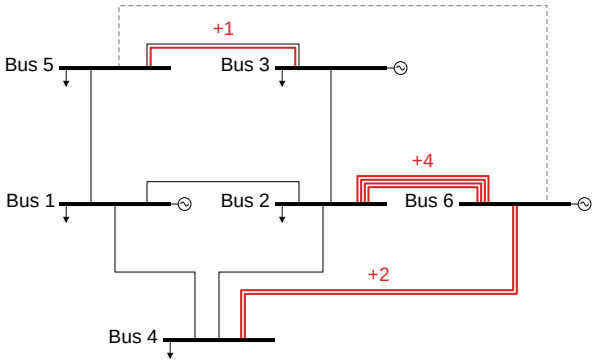
Table 8. Static results on the six-bus Garver system by penetration level: prioritized BTMI-based allocation.

$\bar{\alpha}$	d^{net} (MW)	Prioritized $I(\alpha)$ (USD 1k)	Avoided Cost $C^{\text{av}}(\alpha)$ (USD 1k)
0%	760	1000	0
10%	684	850	150
20%	608	700	300
30%	532	550	450
40%	456	450	550
50%	380	300	700

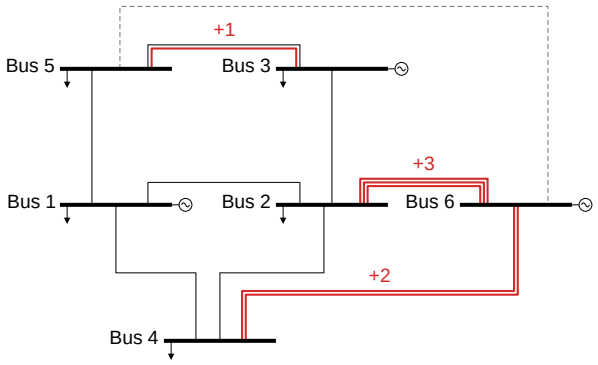
Figure 4 shows the plan behind each row of Table 7 under the uniform allocation, and it reveals three features that reappear later on the real network. The first is that the cost falls in steps, because what leaves the plan is a whole circuit: at 10%, one of the four circuits of corridor 2–6 is no longer needed (panel c). The second is that the composition of the plan does not shrink monotonically even though its cost does. At 20%, the two circuits of corridor 4–6 disappear, but corridor 2–6 returns to four circuits and carries the output of bus 6 on its own (panel d); at 30%, one circuit of 4–6 comes back and 2–6 drops to three, a different plan with the same cost of USD 700k (panel e); and at 40%, the model abandons corridors 2–6 and 3–5 altogether and connects the remote generator through three circuits on 4–6 (panel f). Each penetration level therefore produces its own optimal topology, not a trimmed version of the previous one. The third feature is the value of siting: at 30%, the uniform allocation is still short of removing another circuit, while the prioritized BTMI-based allocation, by concentrating the same aggregate penetration on the importing buses 2, 5 and 4, removes one more and reaches USD 550k (Figure 5e). At 40% and 50%, several plans share the optimal cost; the figures show the one returned by the solver.



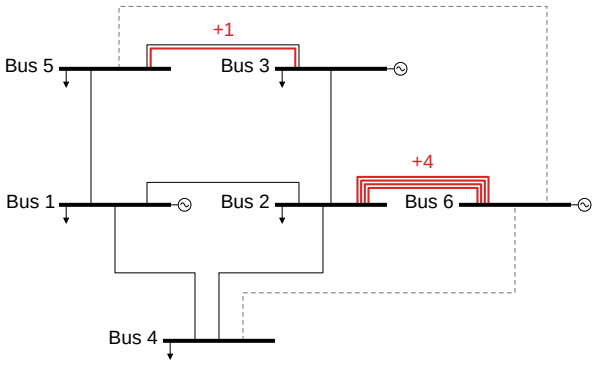
(**a**) Single-line diagram of the Garver test system



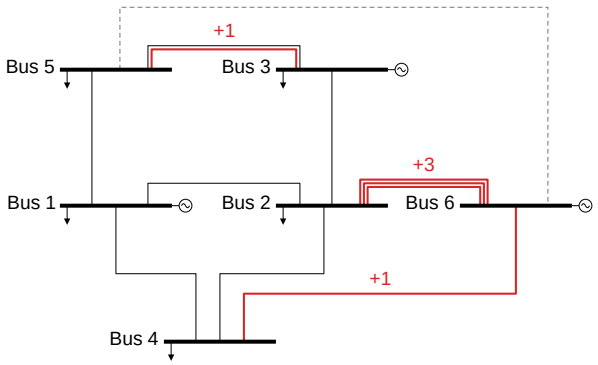
(**b**) $\bar{\alpha} = 0\%$, USD 1000k



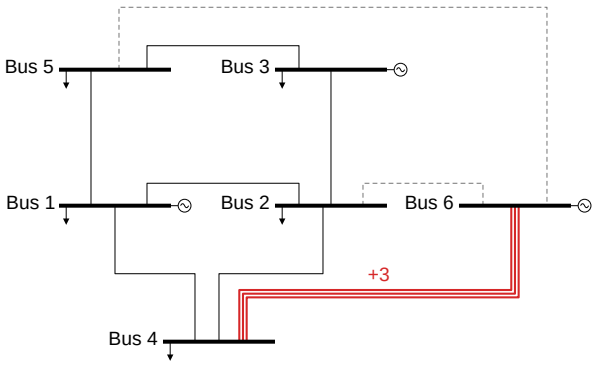
(**c**) $\bar{\alpha} = 10\%$, USD 850k



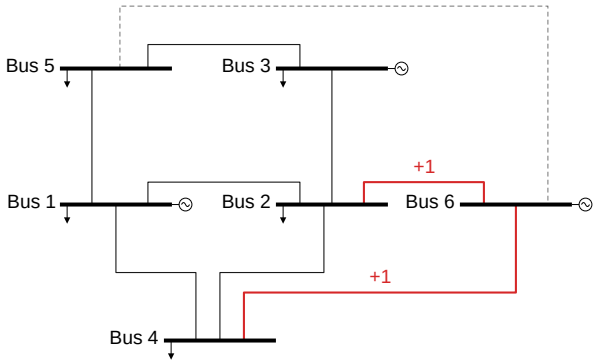
(**d**) $\bar{\alpha} = 20\%$, USD 700k



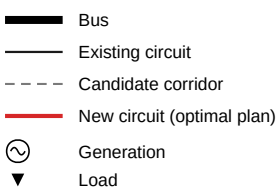
(**e**) $\bar{\alpha} = 30\%$, USD 700k



(**f**) $\bar{\alpha} = 40\%$, USD 450k

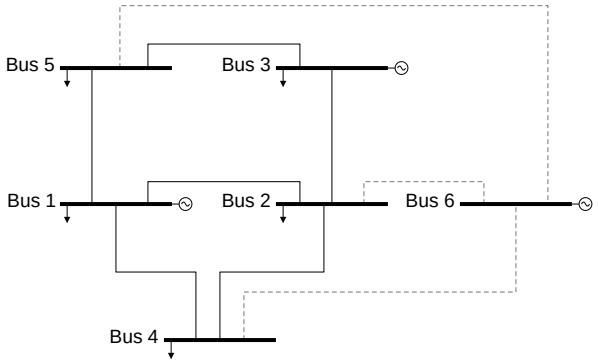


(**g**) $\bar{\alpha} = 50\%$, USD 300k

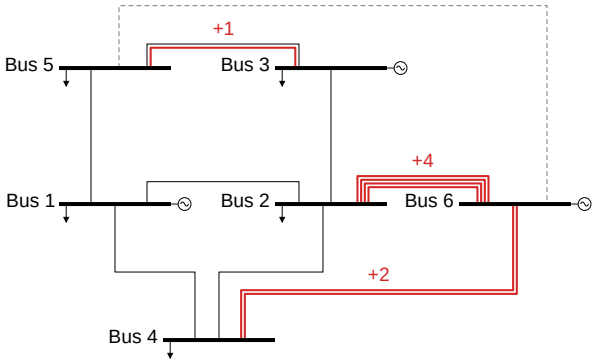


Legend

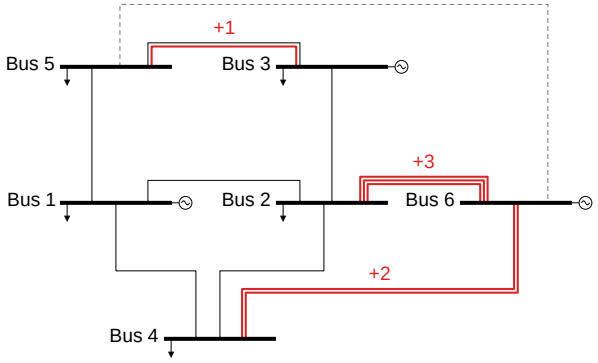
Figure 4. Optimal expansion plans of the Garver system for each BTM penetration level $\bar{\alpha}$ under the uniform allocation strategy. Existing circuits denoted in black, candidate corridors not built in gray dashed lines and new circuits in red, with the number added to each corridor.



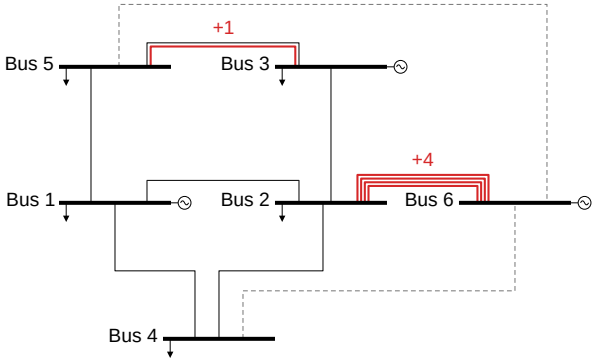
(**a**) Single-line diagram of the Garver test system



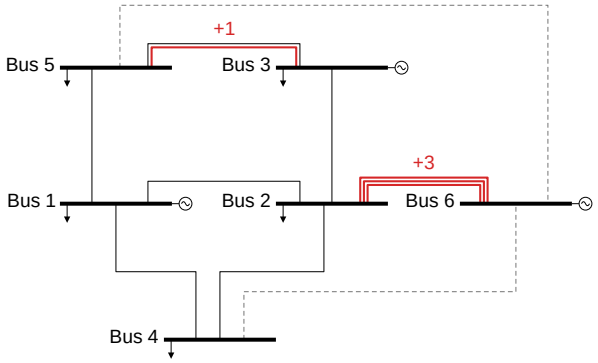
(**b**) $\bar{\alpha} = 0\%$, USD 1000k



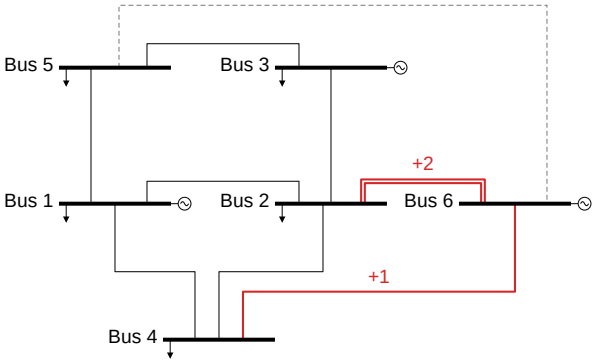
(**c**) $\bar{\alpha} = 10\%$, USD 850k



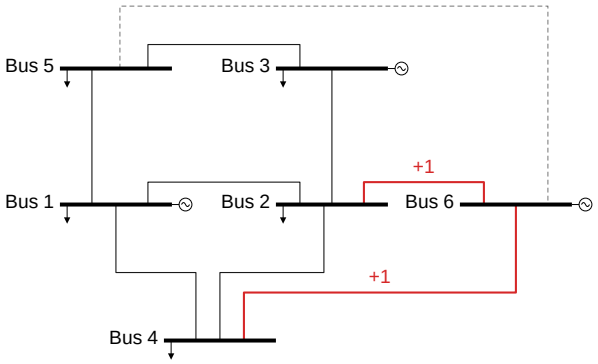
(**d**) $\bar{\alpha} = 20\%$, USD 700k



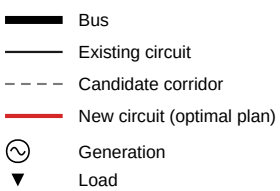
(**e**) $\bar{\alpha} = 30\%$, USD 550k



(**f**) $\bar{\alpha} = 40\%$, USD 450k



(**g**) $\bar{\alpha} = 50\%$, USD 300k



Legend

Figure 5. Optimal expansion plans of the Garver system for each BTM penetration level $\bar{\alpha}$ under the prioritized BTMI-based allocation strategy. Existing circuits denoted in black, candidate corridors not built in gray dashed lines and new circuits in red, with the number added to each corridor.

Over a ten-year horizon with the same 10% discount rate, the multi-period model on the same system produces a base plan with a present value of USD 823k, which falls to USD 730k at a final penetration of 10% and to USD 643k at 20%, that is, deferred credits of USD 93k and 180k. The nominal investment falls in steps while the present value falls continuously, because circuits that are still built are pushed toward later periods.

6.2. The Colombian 500 kV Backbone Results

6.2.1. Nodal Ranking

Table 9 reports the index for the ten highest-ranked nodes, and Figure 6 shows it for every node with demand. The ordering is dominated by the two grid-related terms, since irradiation varies by less than a factor of one and a half across the country while the supply deficit and the corridor loading vary by much more.

Table 9. BTM Index of the ten highest-ranked nodes.

Node	Substation	SPI	NSI	GRI	BTM Index (BTMI)
N23	Norte	0.742	1.000	0.463	0.736
N13	Nueva Esperanza	0.742	0.429	1.000	0.725
N18	Sahagún	0.887	1.000	0.191	0.712
N3	Bacatá	0.742	0.529	0.753	0.682
N14	Ocaña	0.774	0.837	0.394	0.679
N20	San Marcos	0.758	0.639	0.511	0.648
N10	La Virginia	0.758	0.205	0.898	0.634
N11	Medellín	0.694	0.874	0.223	0.607
N8	Heliconia	0.694	0.874	0.194	0.598
N1	Alférez	0.758	0.503	0.435	0.585

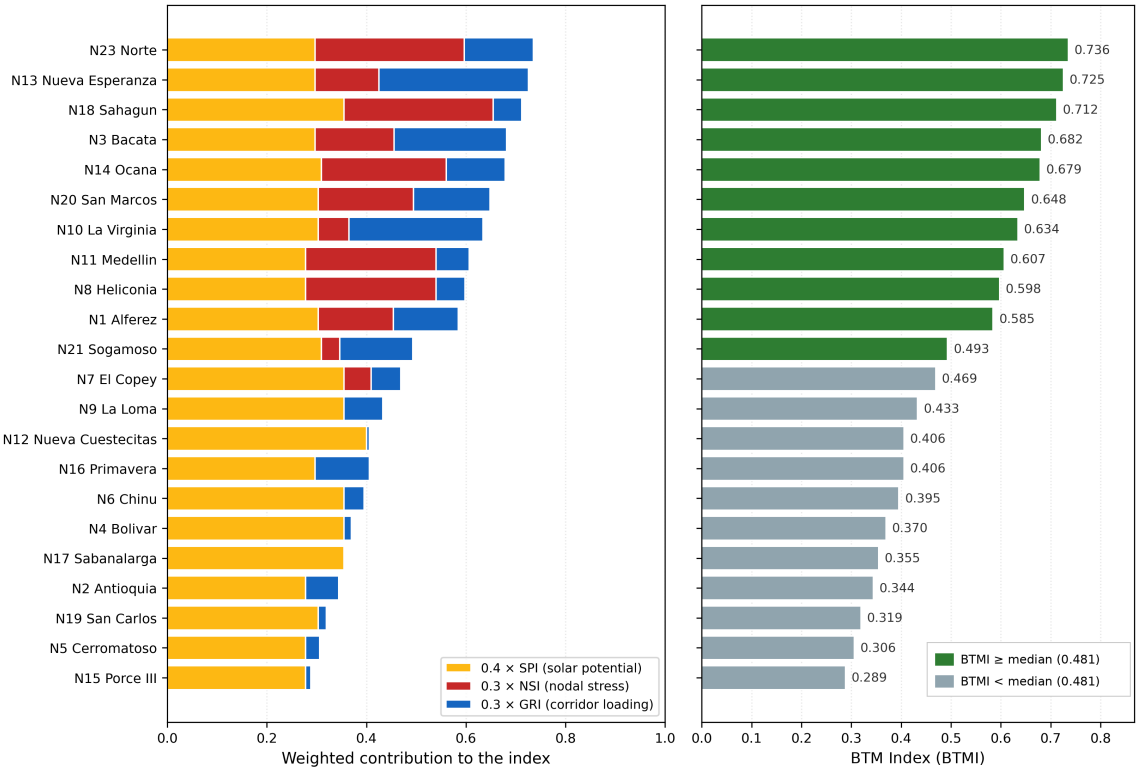


Figure 6. BTM Index by node. (**Left**): decomposition into the SPI, NSI and GRI sub-indices. (**Right**): composite index ordered from highest to lowest.

The result is consistent with the physical reading of the system. The Bogotá-area nodes head the ranking together with Sahagún and Ocaña, all of which combine a large supply deficit with loaded corridors, while the generation hubs sit at the bottom: Porce III scores 0.289, Cerromatoso scores 0.306 and San Carlos scores 0.319. La Guajira is the clearest illustration of why the index cannot be built on the solar resource alone: Nueva Cuestecitas and Colectora have the highest irradiation in the country, and both reach the maximum SPI, yet neither is a priority because there is little or no local demand to reduce.

6.2.2. Base Optimal Expansion Plan

With no behind-the-meter resource, the high-electrification scenario requires five circuits for a total of USD 201.0M, listed in Table 10. Three of them reinforce existing corridors into the Bogotá area and the south-west, one reinforces the internal link of the Bogotá area and one is a candidate project that connects the Norte substation, which is the entry point of the conditioned demand. Figure 7 shows the network and Figure A1 in Appendix B the location of these circuits.

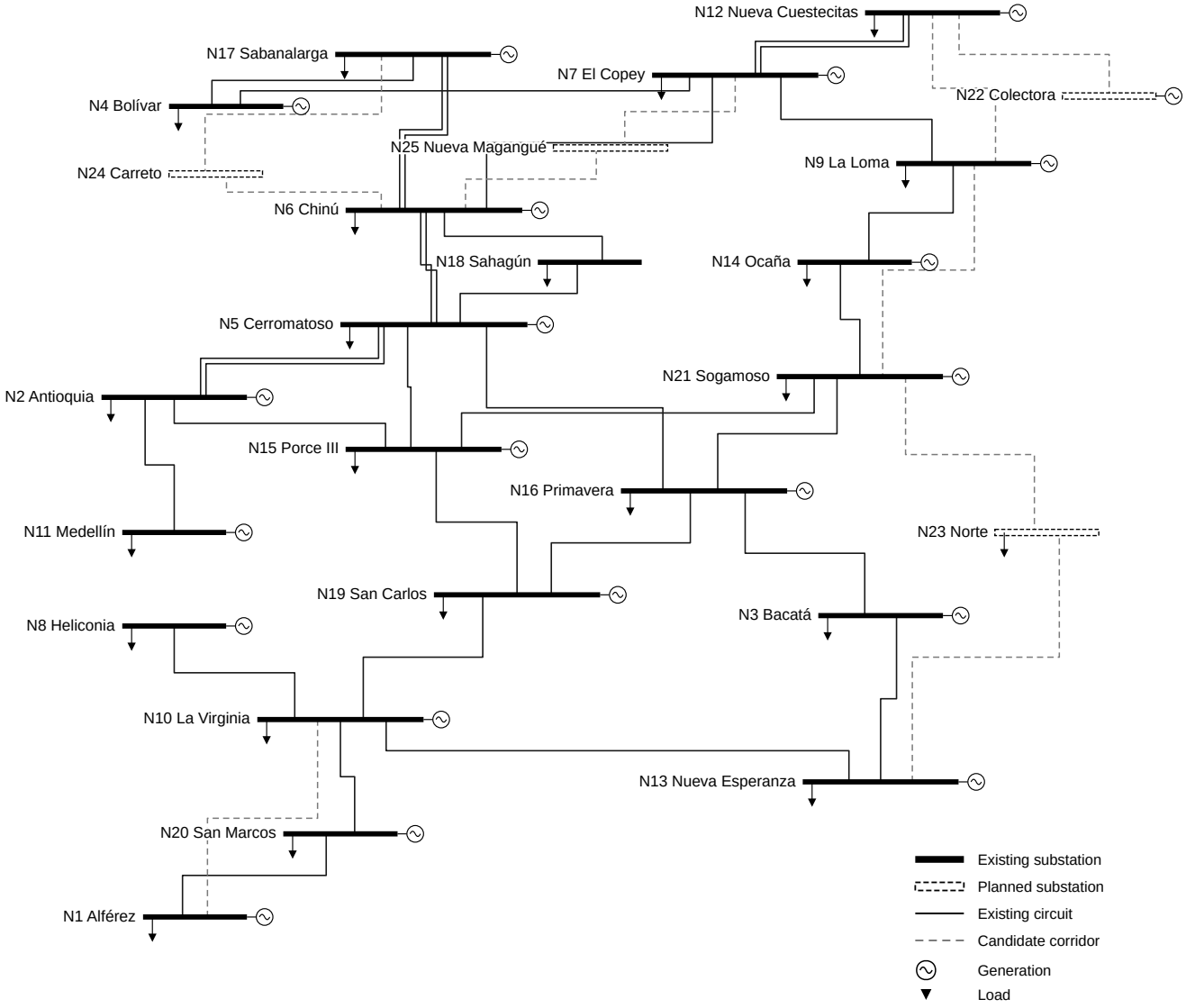


Figure 7. Single-line diagram of the 500 kV backbone equivalent used in the case study. Existing circuits in black and candidate corridors in gray dashed lines. The optimal plan for each penetration level and allocation strategy is shown in Appendix B.

Table 10. Optimal expansion plan without behind-the-meter resource (base).

Corridor	Description	Type	Cost (USD 1M)
N10–N19	La Virginia–San Carlos	reinforcement	60.25
N3–N16	Bacatá–Primavera	reinforcement	55.92
N10–N20	La Virginia–San Marcos	reinforcement	47.08
N13–N23	Nueva Esperanza–Norte	new corridor	24.71
N3–N13	Bacatá–Nueva Esperanza	reinforcement	13.04
Total	5 circuits		201.00

The plan follows the transfer pattern of the scenario. At the target year, the Oriental area needs to import 3487 MW, and the corridors that carry that import, together with those that evacuate the Antioquia and San Carlos hubs toward the south-west, are the ones that saturate: La Virginia–San Carlos and Porce III–San Carlos operate at their rating and Bacatá–Primavera at 98% of it. The plan is therefore not a general reinforcement of the backbone but a targeted one, concentrated at two entry points, which is precisely the condition under which a local demand reduction can be worth a circuit.

6.2.3. Effect of Behind-the-Meter Penetration

Tables 11 and 12 report optimal investment plans for BTM penetrations between 0 and 30% under both allocation strategies, uniform and prioritized.

Table 11. Optimal investment and savings by penetration level: uniform allocation.

$\bar{\alpha}$	d^{net} (MW)	Uniform $I(\alpha)$ (USD 1M)	Avoided Cost $C^{\text{av}}(\alpha)$ (USD 1M)
0%	27,925	201.0	0
5%	26,529	140.9	60.1
10%	25,133	133.2	67.8
15%	23,736	133.2	67.8
20%	22,340	80.6	120.4
25%	20,944	73.0	128.0
30%	19,548	24.7	176.3

Table 12. Optimal investment and savings by penetration level: prioritized BTMI-based allocation.

$\bar{\alpha}$	d^{net} (MW)	Prioritized $I(\alpha)$ (USD 1M)	Avoided Cost $C^{\text{av}}(\alpha)$ (USD 1M)
0%	27,925	201.0	0
5%	26,529	140.9	60.1
10%	25,133	133.2	67.8
15%	23,736	85.0	116.0
20%	22,340	73.0	128.0
25%	20,944	24.7	176.3
30%	19,548	24.7	176.3

The cost trajectory is monotone and stepwise, and Figures A1–A7 in Appendix B show the plan behind each step. A penetration of 5% already removes two of the five circuits, those on Bacatá–Nueva Esperanza and La Virginia–San Marcos, and saves USD 60.1M (Figure A2): a 5% reduction in net demand removes 30% of the plan, six times its own magnitude, which is the clearest expression of the discrete nature of the mechanism. Between 10 and 15% the uniform allocation stalls at USD 133.2M and the plan does not change at all (Figures A3 and A4), because the next circuit is not yet within reach; the prioritized BTMI-based allocation, which concentrates the reduction on the Bogotá and south-western nodes, drops to USD 85.0M at 15%.

Every plan in Figures A1–A7 contains a circuit that connects the Norte substation, and this sets a floor that no penetration removes. That circuit is not there to relieve a transfer: Norte has no other link to the backbone and has to serve the conditioned demand of the area. Behind-the-meter resources reduce the amount of power the network transports, so they can remove reinforcements, but they cannot remove the connection of new load. At 30%, only the shortest connection, from Nueva Esperanza at USD 24.7M, remains (Figure A7), and the credit saturates at USD 176.3M, 88% of the base plan, rather than at its full value.

Figures A9–A15 in Appendix B show the plans under the prioritized BTMI-based allocation and Figure 8 compares both cost trajectories. The comparison is less regular than the intuition suggests. In the cases evaluated, the prioritized BTMI-based allocation was not worse than the uniform allocation at any penetration level, and its advantage over the uniform allocation reaches USD 48.2M at 15% and USD 48.3M at 25%, close to the cost of a full circuit in each case, while at 20% it is only USD 7.6M and at the remaining levels, the two coincide. The reason is that both allocations sometimes fall on the same side of the threshold where a circuit leaves the plan. The value of siting is thus real but discrete: it materializes when the concentration of the reduction is enough to cross a threshold that the uniform allocation does not reach, and it vanishes when both cross it or neither does.

The plans of the uniform allocation also show that, as in the Garver system, the plan is re-optimized rather than trimmed. At 10%, the connection of Norte moves from Nueva Esperanza to Sogamoso (Figure A3). The longer circuit costs USD 73.0M, but it brings power into the Bogotá area through a new path and relieves Bacatá–Primavera, so it does the job of two circuits that together cost USD 80.6M. At 20%, the reinforcement of La Virginia–San Carlos leaves the plan and the cheapest combination returns to the Nueva Esperanza connection with Bacatá–Primavera (Figure A5); at 25%, the Sogamoso connection alone is enough (Figure A6); and at 30%, only the short connection from Nueva Esperanza remains. Bacatá–Primavera thus leaves the plan at 10% and comes back at 20%, which a method that removes circuits from a fixed base plan could not reproduce.

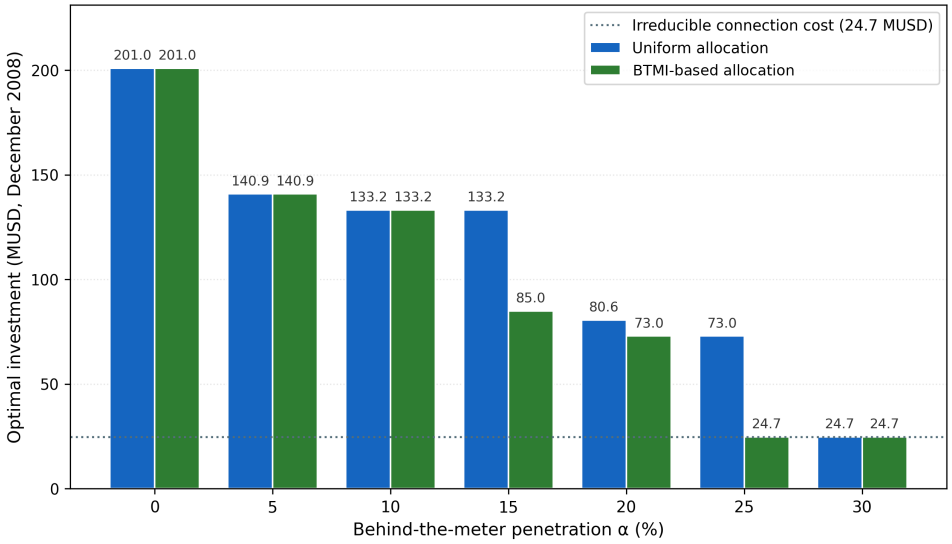


Figure 8. Optimal investment as a function of BTM penetration factor $\bar{\alpha}$ under the uniform and prioritized BTMI-based allocations.

6.2.4. Multi-Period Results and Deferred Credit

The multi-period model answers when each circuit is needed, and therefore separates what is avoided from what is only postponed. Table 13 reports the results for final penetrations of 10 and 20% under the uniform allocation.

Table 13. Multi-period results over the 2026–2040 horizon, uniform allocation.

Scenario	Nominal (USD 1M)	NPV (USD 1M)	Deferred Credit (USD 1M)	Reduction (%)
Base, $\bar{\alpha} = 0$	201.0	90.8	–	–
$\bar{\alpha} = 10\%$	140.9	65.8	24.9	27.5
$\bar{\alpha} = 20\%$	80.6	42.1	48.7	53.7

The schedule in Table 14 and Figure 9 shows where the credit comes from. In every scenario the connection of the Norte substation is built in 2027, which confirms that this element is driven by load connection and not by transfer. The reinforcement of La Virginia–San Carlos moves from 2033 to 2035 when penetration reaches 10% and disappears at 20%. Bacatá–Primavera moves from 2036 to 2038 and then to 2037 in the scenario where it is the only reinforcement left. The two circuits that the base plan builds in 2040 are not built within the horizon under either penetration.

Table 14. Annual investment of the multi-period plan (USD 1M). Only years with investment are shown.

Year	$\bar{\alpha} = 0$	$\bar{\alpha} = 10\%$	$\bar{\alpha} = 20\%$
2027	24.7	24.7	24.7
2033	60.3	–	–
2035	–	60.3	–
2036	55.9	–	–
2037	–	–	55.9
2038	–	55.9	–
2040	60.1	–	–

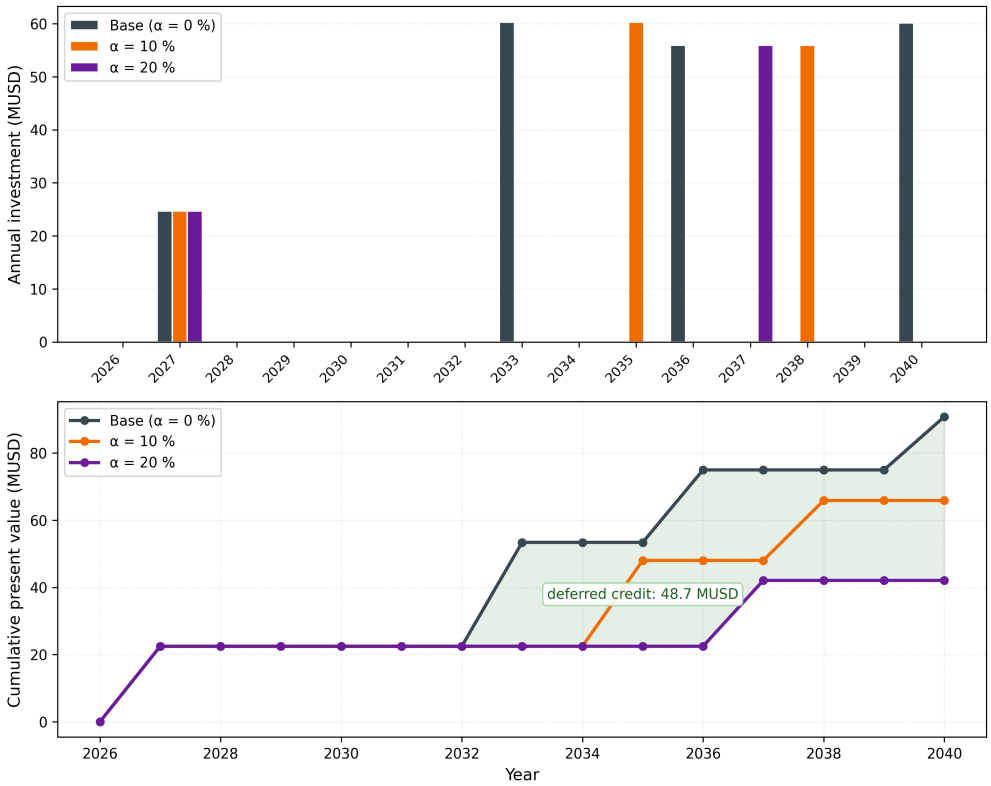


Figure 9. Multi-period plan for each final penetration level $\bar{\alpha}$. (**Top**): annual investment. (**Bottom**): cumulative present value, where the shaded area is the deferred credit.

The deferred credit therefore has the two components it is supposed to have. Part of it is investment that leaves the plan altogether, and part is investment that is still made but one to two years later, which the discount rate turns into a present-value saving. The relation between penetration and credit remains monotone in present value. The reduction in the present value, 27.5% and 53.7% of the base value, is somewhat smaller than the reduction in the nominal plan, 30% and 60%, respectively.

6.3. Magnitude of the Results and Monetary Base

The figures reported above are expressed in December 2008 US dollars, which is the base of the reference construction units used to cost the circuits [62]. Two implications follow. First, the plan of USD 201M is not comparable to the budget of a project tendered today; an escalation to current dollars would raise it by roughly the accumulated inflation of the period. Second, and more usefully for the purposes of this paper, the escalation is a single multiplicative factor applied to every corridor, because all of them are costed with the same unit prices. Indexing would therefore scale the base plan, the savings and the deferred credit by the same amount, and would leave unchanged the share of the plan that each penetration level removes, the comparison between the two allocation strategies and the shape of the credit curve. The results should be read as relative magnitudes, which is also how they are used: a penetration of 5% removes 30% of the plan, and a final penetration of 20% removes slightly more than half of its present value.

6.4. Limitations

Security criterion. For the sake of simplicity, no N-1 criterion is imposed, so the plans are the minimum set of circuits for normal operation. An N-1 study would yield a larger base plan and most likely a larger credit, since relieving a corridor is worth more when its secure capacity is smaller. The absolute figures may therefore be conservative, although only an N-1 study could confirm it. The deterministic MILP-DC model was adopted to isolate and illustrate the deferral credit as a function of BTM penetration; stochastic TEP methods, such as Monte Carlo simulation, point estimate methods or scenario-based stochastic and robust optimization [28,29,31], can replace it to capture the variability of the solar resource and of BTM storage without changing the definition of the credit.

Dimensioning condition. BTM generation level α_i is applied to each nodal peak demand, typically at night, and assumes a firm BTM generation at that hour from storage or other small-scale sources. For PV without storage the credit is an upper bound. The model does not require the network to supply the gross demand d_i if the BTM resources become unavailable; this backup requirement is assumed to be limited because the aggregate output of many small units is more predictable than that of a single plant. If the daytime demand exceeded the night-time peak, the daytime condition would size the network and should be studied separately. The variability of the resource (cloudy days, inter-annual variation) requires stochastic scenarios and is left for future work.

Irradiation premise. The link between the penetration factor α_i and irradiation holds where PV with storage dominates; elsewhere, the solar potential index should be replaced by an index of the dominant resource, without changing the rest of the method. Deployment also depends on tariffs, income, housing and regulation, so the correlation is expected to be positive but not strong. In Colombia, its effect is limited, because irradiation varies by less than a factor of 1.5 and the ranking is driven by the grid terms.

Penetration granularity. The penetration level $\bar{\alpha}$ is evaluated in steps of 5 or 10 percentage points. Since the investment changes in discrete steps, the exact thresholds at which a circuit leaves the plan or is postponed lie between the evaluated levels, and a finer evaluation

around those transitions, together with the sensitivity of the savings to small deviations from the assumed penetration, is left for future work. This does not change the qualitative findings: the reduction is stepwise, location-dependent and bounded by the connection of new load.

Dispatch and penetration. Central generation is dispatched without cost, which may differ from the market dispatch. BTM generation, in turn, is self-dispatched at no cost and does not take part in the hourly matching of supply and demand that sets prices: prosumers are price-takers. A special case is that of large data centers of hundreds of MW, which are also BTM users but are connected to the transmission network and must sell their surpluses in the spot or financial markets; their output would then follow market signals rather than the exogenous penetration assumed here. The penetration factor is assigned exogenously: the models measure what a given penetration is worth to the network, not how much BTM generation would be installed. Finally, the multi-period model was solved only under the uniform allocation.

7. Conclusions

This paper proposes a new methodology to assess avoided and deferred investment credits considering the widespread deployment of behind-the-meter (BTM) generation. BTM generation enters the traditional transmission expansion planning problem as a nodal reduction in net demand, and a BTM Index ranks where that reduction is most valuable as an overall avoided or deferred cost that can be passed on to end users through lower network tariffs. Tariffs are not computed in this paper, but the credit is precisely the quantity a regulator needs to pass these savings on: it measures the transmission investment that the BTM resource avoids or postpones, and the BTMI indicates where it does so.

To the best of our knowledge, this is the first application of the deferred transmission investment credit due to the BTM effect, such as rooftop PV with storage, within a re-optimized transmission plan: previous studies credited resources that inject into the grid, valued marginal load reductions against a fixed plan or assessed distributed solar through system-wide adoption scenarios without a nodal representation or a present-value deferral credit.

- BTM generation, represented as a reduction in net demand, can be interpreted as a virtual transmission resource, and its value can be measured inside a standard expansion model. The methodology requires no change to the network formulation and can be applied to other systems with significant penetration, so the planner can read the avoided and deferred investment directly from the optimal plans.
- The credit is discrete, not proportional. Small penetration levels remove whole circuits: in the Colombian case, a 5% reduction in net demand removes 30% of the plan, while in other intervals additional penetration produces no saving until the next threshold is crossed.
- There is a floor that the resource cannot remove. Behind-the-meter generation reduces what the network transports, not the need to connect new load. The circuit that connects a new load center remains in every plan, so the credit saturates below the full investment, at 88% of the base plan in the Colombian case.
- Location matters, but in steps. Concentrating penetration on the nodes with the highest index was not worse than spreading it uniformly at any of the penetration levels evaluated, and is worth close to a full circuit when it crosses a threshold the uniform allocation does not reach. The priority nodes are loads with a supply deficit and loaded corridors, not the nodes with the best solar resource.

- The credit combines avoided and postponed investment. Over the planning horizon, part of the saving comes from circuits that are not built within the horizon and part from circuits built one to two years later; final penetrations of 10% and 20% reduce the present value of the Colombian plan by 27.5% and 53.7%, respectively.
- The plan is re-optimized, not trimmed. In both systems, each penetration level produces its own optimal plan, and some circuits leave the plan and return at a higher level. Estimates that remove circuits from a fixed base plan miss this effect.
- The results support targeting incentives for energy communities and self-generators by location. A prioritized BTMI-based allocation offers a transparent criterion to direct public resources to the nodes where BTM generation relieves the network the most.

For future assessments, the expansion problem should include the N-1 security criterion, which changes the base plan and the transfer limits that the behind-the-meter resource relieves. The thresholds at which the plan changes should also be located with a finer evaluation of the penetration, and the robustness of the savings to deviations from the assumed penetration assessed within that stochastic framework. Other natural extensions are the subtransmission and transformation levels, the multi-period evaluation of the prioritized BTMI-based allocation, operating costs in the objective and a bi-level formulation that couples expansion planning with the optimal sizing of behind-the-meter generation and storage.

Author Contributions: Conceptualization, J.P.R.O., M.A.R., A.T., S.C. and P.M.D.O.-D.J.; Methodology, J.P.R.O., M.A.R., A.T., S.C. and P.M.D.O.-D.J.; Software, J.P.R.O. and A.J.S.; Validation, M.A.R., A.T. and P.M.D.O.-D.J.; Writing—original draft, J.P.R.O.; Writing—review and editing, M.A.R., A.T., S.C. and P.M.D.O.-D.J.; Supervision, P.M.D.O.-D.J. All authors have read and agreed to the published version of the manuscript.

Funding: This research received no external funding. Internal funding from the School of Engineering supported MS student assistance.

Data Availability Statement: The network data used in this study are publicly available from the sources cited in Section 5. The optimization models and the scripts that reproduce the results are openly available at https://github.com/jrincono/Optimizacion-TEP (accessed on 19 November 2026).

Acknowledgments: During the preparation of this manuscript, the authors used generative AI tools (GPT-6.2 Astra, OpenAI; Claude Opus 5.5, Anthropic) to support language editing and the implementation of the optimization scripts. The authors reviewed and edited all output and take full responsibility for the content of this publication.

Conflicts of Interest: The authors declare no conflict of interest.

Nomenclature

Acronyms

AGGE	Large-scale self-generation (autogeneración a gran escala)
AGPE	Small-scale self-generation (autogeneración a pequeña escala)
BESS	Battery energy storage system
BTM	Behind the meter
BTMI	Behind-the-meter (BTM) index
DC	Direct current (linearized power flow)
DER	Distributed energy resources
DG	Distributed generation
EV	Electric vehicles
GHI	Global horizontal irradiation
GRI	Grid reinforcement index

MILP	Mixed-integer linear programming
NPV	Net present value
NSI	Nodal stress index
NWA	Non-wires alternatives
PV	Photovoltaic
SPI	Solar potential index
TEP	Transmission expansion planning
USD 1k/1M	Thousands/millions of US dollars

Sets and indices

$\mathcal{I}$	Set of nodes, indexed by i
$\mathcal{J}$	Set of corridors, indexed by j
$\mathcal{K}$	Set of circuit positions per corridor, indexed by k
$\mathcal{T}$	Set of periods, indexed by t
Ω_i	Set of corridors incident to node i
a, b	Sending and receiving ends of corridor j

Parameters

B_j	Susceptance of corridor j (p.u.)
c_j	Cost of one circuit of corridor j (USD 1M)
d_i	Nodal peak power demand at node i (MW)
d_i^{net}	Net demand at node i (MW)
d_i^{trend}	Trend demand at node i (MW)
l_i^{conc}	Concentrated loads without their own generation at node i (MW)
d_i^{EV}	Demand of electric vehicles at node i (MW)
g_i^{BTM}	BTM generation at node i at the peak hour (MW)
$F_j^{\max}$	Thermal rating of one circuit of corridor j (MW)
$G_i^{\max}$	Generation capacity available at node i (MW)
GHI_i	Daily global horizontal irradiation at node i (kWh/m^2 per day)
M_j	Disjunctive constant of corridor j (p.u.)
n_j^0	Circuits of corridor j already in service
n	Number of nodes
r	Discount rate
S_{ij}	Node-corridor incidence
T	Number of periods
X_j	Reactance of corridor j (p.u.)
α_i	Behind-the-meter penetration fraction at node i
$\alpha_{i,t}$	Behind-the-meter penetration at node i in period t
α	Penetration vector, $\alpha = [\alpha_1, \ldots, \alpha_n]$
$\alpha^{\max}$	Maximum penetration allowed at a node
$\bar{\alpha}$	Aggregate penetration level, mean of α
Γ	Investment budget (USD 1M)
$\Delta\theta^{\max}$	Bound on the angular difference between nodes (rad)
$\hat{f}_j$	Flow of corridor j in the base case (MW)
η_N, η_G	Normalization factors of the NSI and GRI sub-indices
SPI_i	Solar potential index of node i
NSI_i	Nodal stress index of node i
GRI_i	Grid reinforcement index of node i
$BTMI_i$	Behind-the-meter index of node i
$\overline{BTMI}$	Mean BTM index over the nodes with demand

Variables

$f_{j,k}$	Power flow through circuit k of corridor j (p.u.)
g_i	Power injected at node i (p.u.)
$x_{j,k,t}$	1 if circuit k of corridor j is available in period t
$y_{j,k}$	1 if circuit k of corridor j is in service (static model)
$y_{j,k,t}$	1 if circuit k of corridor j is built in period t
θ_i	Voltage angle at node i (rad)

Metrics

$C^{\text{av}}(\alpha)$	Avoided investment (USD 1M)
$C^{\text{def}}(\alpha)$	Deferred investment credit in present value (USD 1M)
I^{base}	Cost of the optimal plan without behind-the-meter resource (USD 1M)
I_t	Investment committed in period t (USD 1M)
$I(\alpha)$	Cost of the optimal plan under penetration vector α (USD 1M)

Appendix A. Test System Data

Appendix A.1. Garver System

Table A1 lists the corridor data of the six-bus system. Demand and generation capacity are given in Table 4 of the main text. Corridors with no assigned cost are not candidates in this variant of the problem.

Table A1. Corridor data of the Garver system.

Corridor	Existing Circuits	B_j (p.u.)	$F_j^{\max}$ (MW)	c_j (USD 1k)
1–2	1	2.50	100	–
1–3	0	–	100	–
1–4	1	1.67	80	–
1–5	1	5.00	100	–
1–6	0	–	70	–
2–3	1	5.00	100	–
2–4	1	2.50	100	–
2–5	0	–	100	–
2–6	0	3.33	100	150
3–4	0	–	82	–
3–5	1	5.00	100	100
3–6	0	–	100	–
4–5	0	–	75	–
4–6	0	3.33	100	150
5–6	0	1.64	78	350

Appendix A.2. Colombian 500 kV Backbone

Table A2 lists the 37 corridors of the equivalent network, 27 of them already in service with 31 circuits and 10 associated with planned projects. Reactances are expressed on a 100 MVA base, ratings correspond to the average of the circuits of the corridor, and costs are per circuit in December 2008 US dollars. Nodal demand and generation are given in Table 5 of the main text.

Table A2. Corridor data of the 500 kV backbone.

Corridor	Substations	n_j^0	Length (km)	X_j (p.u.)	$F_j^{\max}$ (MW)	c_j (USD 1M)
N1–N20	Alférez–San Marcos	1	36	0.0046	2078	10.22
N2–N5	Antioquia–Cerromatoso	2	113	0.0144	2078	31.97
N2–N11	Antioquia–Medellín	1	110	0.0141	2078	31.12
N2–N15	Antioquia–Porce III	1	113	0.0145	2078	32.03
N3–N13	Bacatá–Nueva Esperanza	1	46	0.0064	2165	13.04
N3–N16	Bacatá–Primavera	1	197	0.0261	1650	55.92
N4–N7	Bolívar–El Copey	1	167	0.0223	1650	43.33
N4–N17	Bolívar–Sabanalarga	1	67	0.0085	2078	17.30
N5–N6	Cerromatoso–Chinú	2	134	0.0171	2122	38.13
N5–N15	Cerromatoso–Porce III	1	142	0.0187	1650	40.23
N5–N16	Cerromatoso–Primavera	1	245	0.0316	2165	69.64
N5–N18	Cerromatoso–Sahagún	1	79	0.0110	2078	22.46
N6–N7	Chinú–El Copey	1	233	0.0290	2078	60.46
N6–N17	Chinú–Sabanalarga	2	184	0.0243	2111	47.80
N6–N18	Chinú–Sahagún	1	53	0.0074	2078	13.78
N7–N9	El Copey–La Loma	1	73	0.0104	1650	18.98
N7–N12	El Copey–Nueva Cuestecitas	2	218	0.0270	2078	56.74
N8–N10	Heliconia–La Virginia	1	178	0.0231	2078	50.69

Table A2. *Cont.*

Corridor	Substations	n_j^0	Length (km)	X_j (p.u.)	$F_j^{\max}$ (MW)	c_j (USD 1M)
N9–N14	La Loma–Ocaña	1	168	0.0239	1650	47.71
N10–N13	La Virginia–Nueva Esperanza	1	238	0.0305	2078	67.47
N10–N19	La Virginia–San Carlos	1	212	0.0268	1732	60.25
N10–N20	La Virginia–San Marcos	1	166	0.0210	1732	47.08
N14–N21	Ocaña–Sogamoso	1	164	0.0216	1650	46.49
N15–N19	Porce III–San Carlos	1	106	0.0140	1650	30.24
N15–N21	Porce III–Sogamoso	1	236	0.0299	2078	66.94
N16–N19	Primavera–San Carlos	1	83	0.0107	2165	23.47
N16–N21	Primavera–Sogamoso	1	136	0.0180	1650	38.53
N1–N10	Alférez–La Virginia	0	183	0.0237	2078	51.97
N6–N24	Chinú–Carreto	0	180	0.0233	2078	46.79
N6–N25	Chinú–Nueva Magangué	0	95	0.0123	2078	24.69
N7–N25	El Copey–Nueva Magangué	0	140	0.0181	2078	36.39
N9–N12	La Loma–Nueva Cuestecitas	0	220	0.0285	2078	57.19
N9–N21	La Loma–Sogamoso	0	275	0.0356	2078	78.10
N12–N22	Nueva Cuestecitas–Colectora	0	220	0.0285	2078	57.19
N13–N23	Nueva Esperanza–Norte	0	87	0.0113	2078	24.71
N17–N24	Sabanalarga–Carreto	0	110	0.0142	2078	28.59
N21–N23	Sogamoso–Norte	0	257	0.0332	2078	72.99

Appendix B. Expansion Plans of the 500 kV Backbone

This appendix shows, at full page, the optimal expansion plan of the 500 kV backbone for each behind-the-meter penetration level $\bar{\alpha}$ discussed in Section 6. Figures A1–A7 correspond to the uniform allocation and Figures A8–A15 to the BTMI allocation.

Appendix B.1. Uniform Allocation

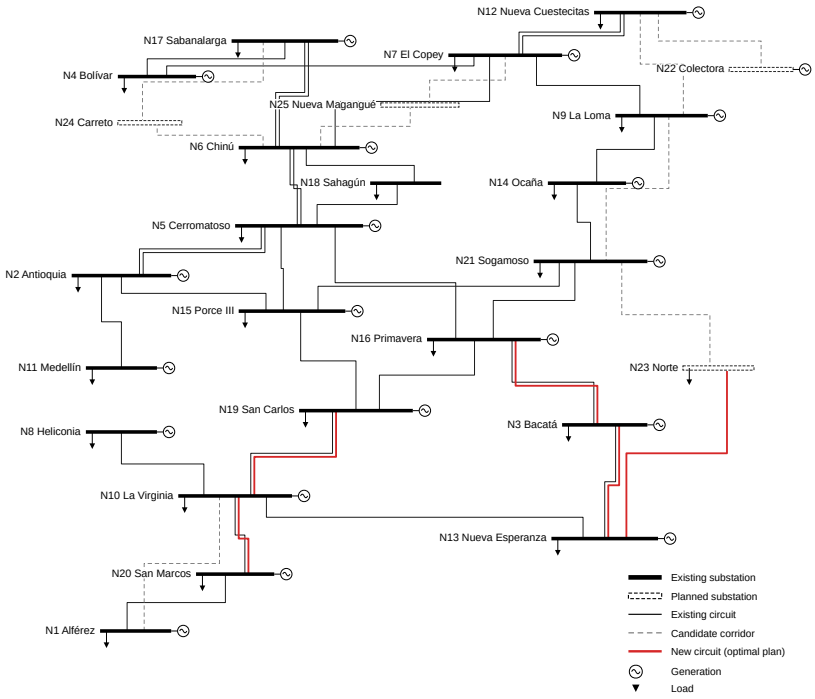


Figure A1. Optimal expansion plan of the 500 kV backbone under the uniform allocation, $\bar{\alpha} = 0\%$, USD 201.0M. Existing circuits in black, candidate corridors not built in gray dashed lines, and new circuits, including reinforcements of existing corridors, in red.

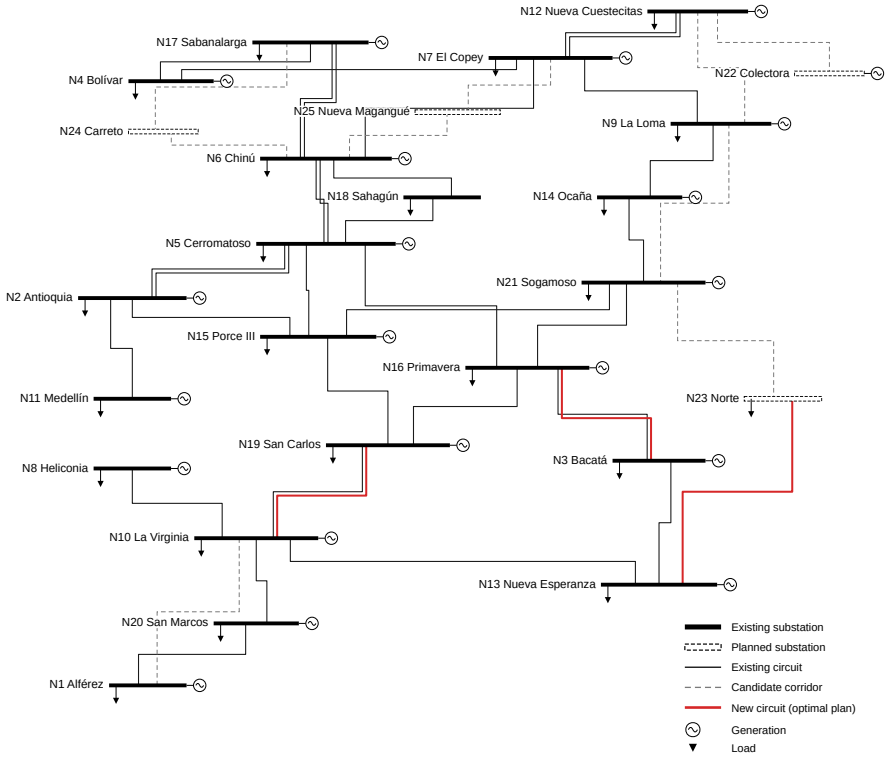


Figure A2. Optimal expansion plan of the 500 kV backbone under the uniform allocation, $\bar{\alpha} = 5\%$, USD 140.9M. Existing circuits in black, candidate corridors not built in gray dashed lines and new circuits, including reinforcements of existing corridors, in red.

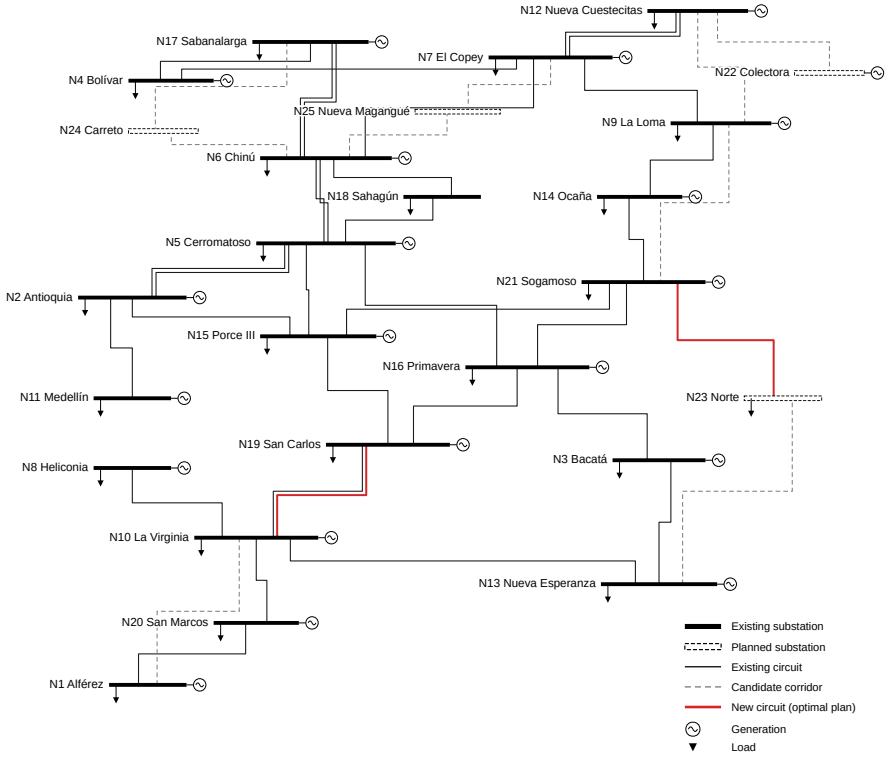


Figure A3. Optimal expansion plan of the 500 kV backbone under the uniform allocation, $\bar{\alpha} = 10\%$, USD 133.2M. Existing circuits in black, candidate corridors not built in gray dashed lines and new circuits, including reinforcements of existing corridors, in red.

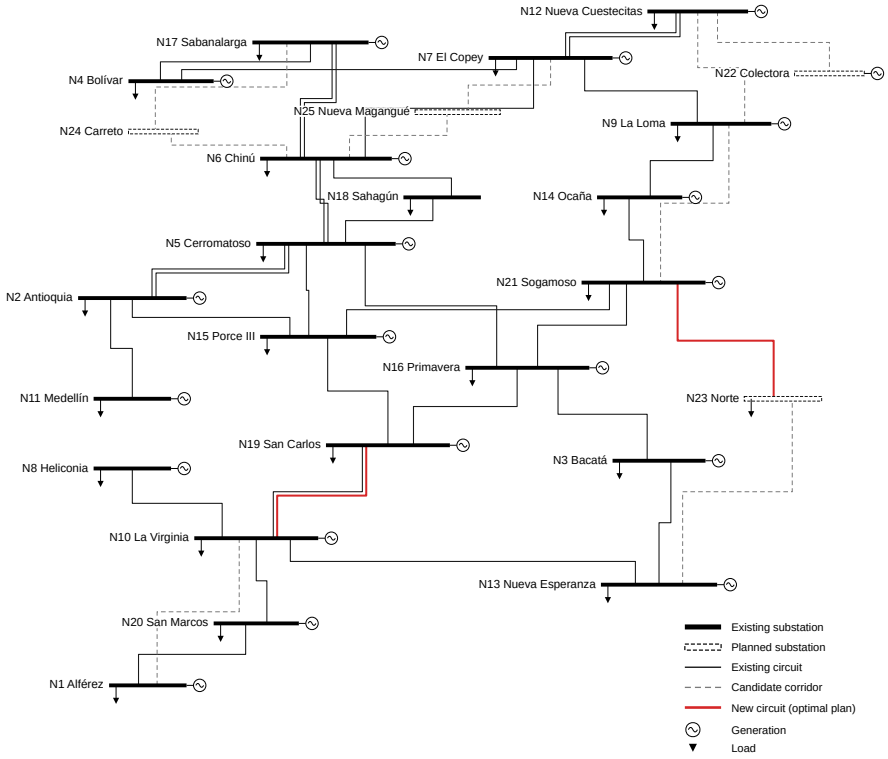


Figure A4. Optimal expansion plan of the 500 kV backbone under the uniform allocation, $\bar{\alpha} = 15\%$, USD 133.2M. Existing circuits in black, candidate corridors not built in gray dashed lines and new circuits, including reinforcements of existing corridors, in red.

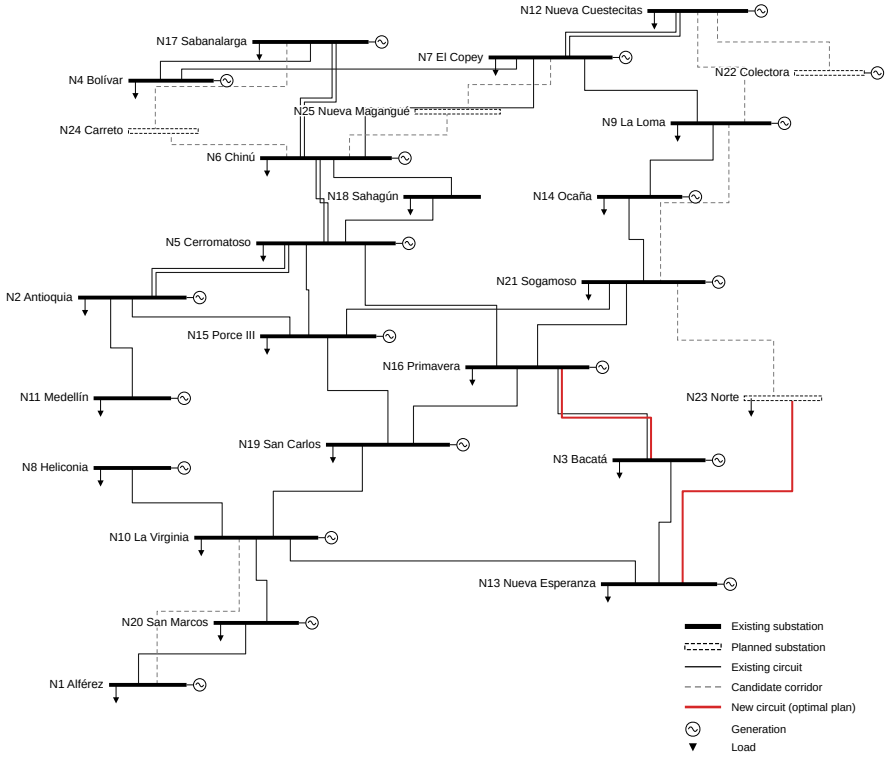


Figure A5. Optimal expansion plan of the 500 kV backbone under the uniform allocation, $\bar{\alpha} = 20\%$, USD 80.6M. Existing circuits in black, candidate corridors not built in gray dashed lines and new circuits, including reinforcements of existing corridors, in red.

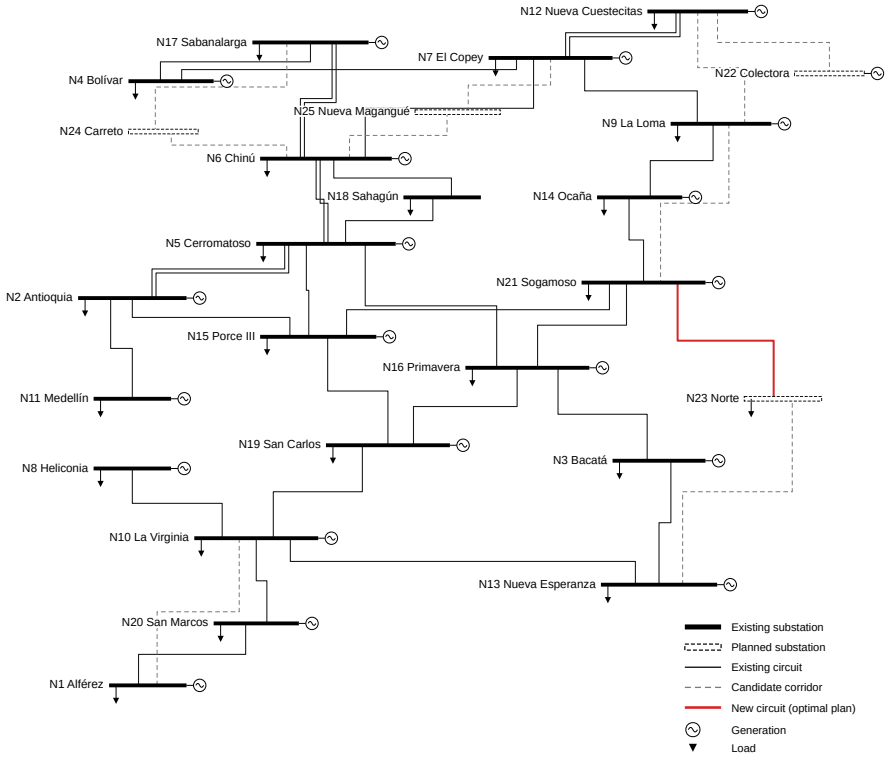


Figure A6. Optimal expansion plan of the 500 kV backbone under the uniform allocation, $\bar{\alpha} = 25\%$, USD 73.0M. Existing circuits in black, candidate corridors not built in gray dashed lines and new circuits, including reinforcements of existing corridors, in red.

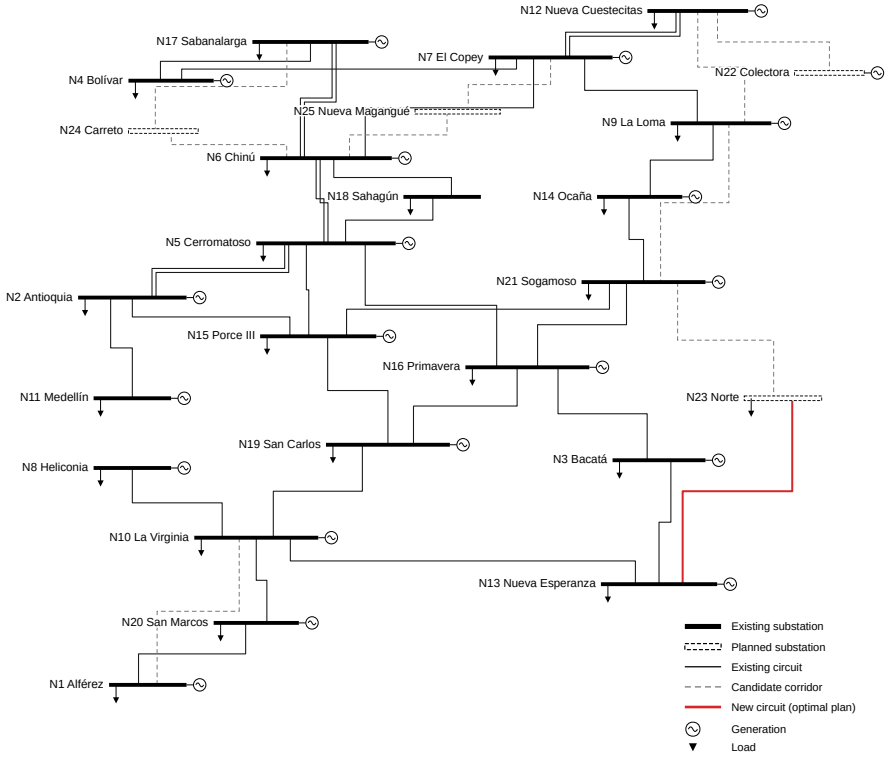


Figure A7. Optimal expansion plan of the 500 kV backbone under the uniform allocation, $\bar{\alpha} = 30\%$, USD 24.7M. Existing circuits in black, candidate corridors not built in gray dashed lines and new circuits, including reinforcements of existing corridors, in red.

Appendix B.2. BTMI-Based Allocation

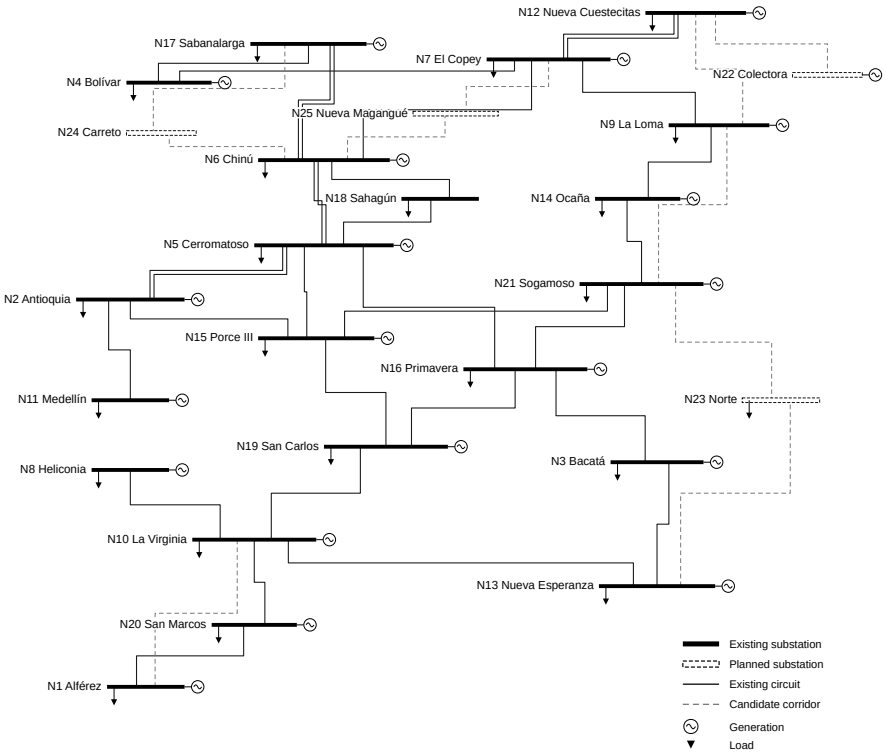


Figure A8. Single-line diagram of the 500 kV backbone equivalent used in the case study (reference for the BTMI-based allocation). Existing circuits in black and candidate corridors in gray dashed lines.



Figure A9. Optimal expansion plan of the 500 kV backbone under the BTMI allocation, $\bar{\alpha} = 0\%$, USD 201.0M. Existing circuits in black, candidate corridors not built in gray dashed lines and new circuits, including reinforcements of existing corridors, in red.

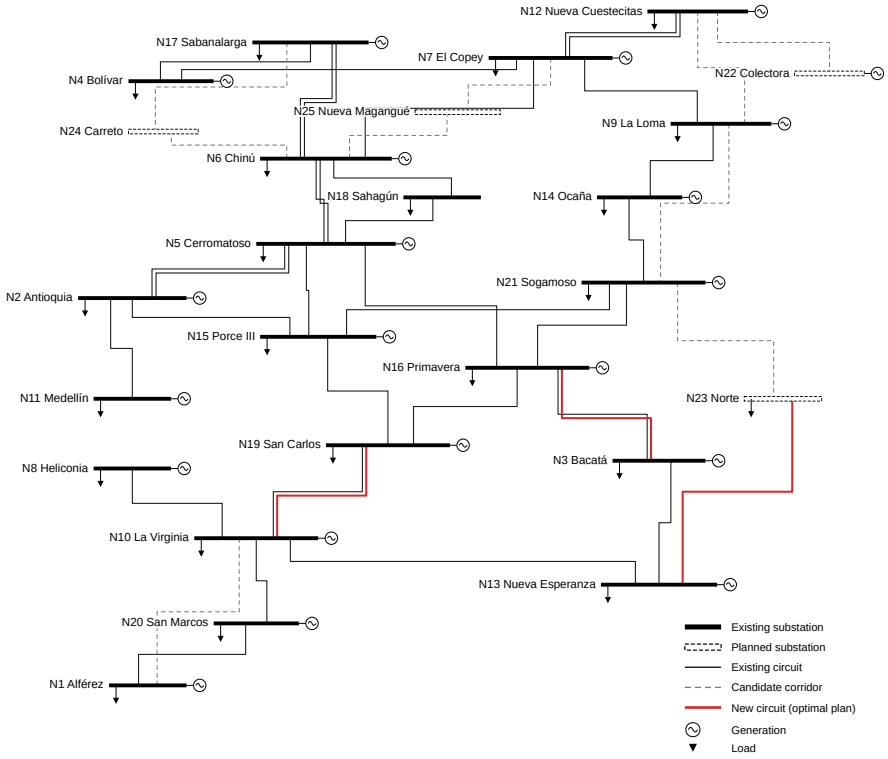


Figure A10. Optimal expansion plan of the 500 kV backbone under the BTMI allocation, $\bar{\alpha} = 5\%$, USD 140.9M. Existing circuits in black, candidate corridors not built in gray dashed lines and new circuits, including reinforcements of existing corridors, in red.

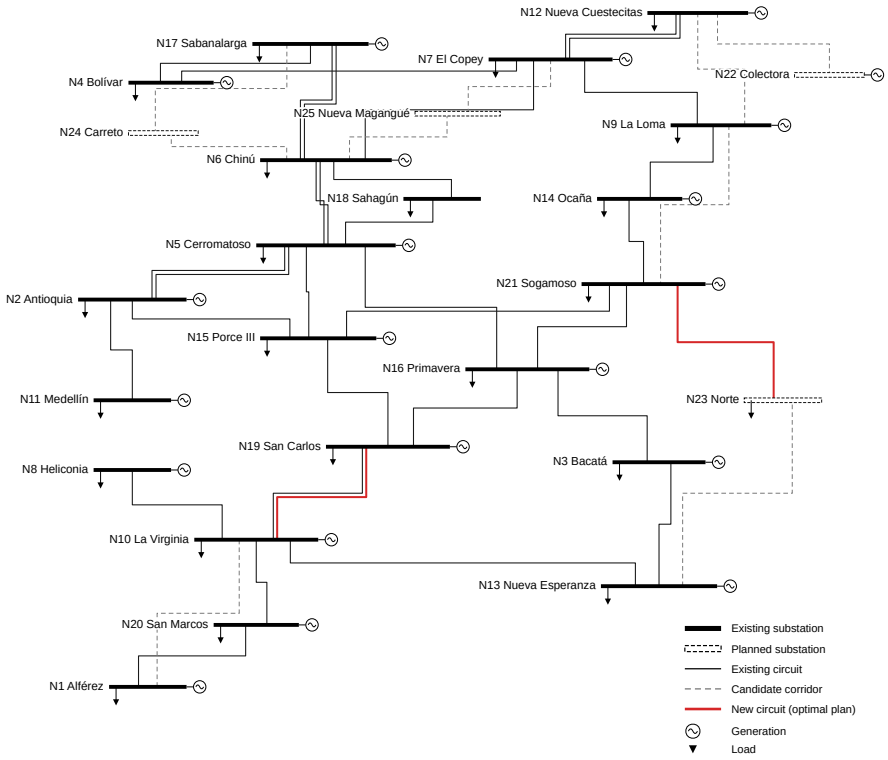


Figure A11. Optimal expansion plan of the 500 kV backbone under the BTMI allocation, $\bar{\alpha} = 10\%$, USD 133.2M. Existing circuits in black, candidate corridors not built in gray dashed lines and new circuits, including reinforcements of existing corridors, in red.

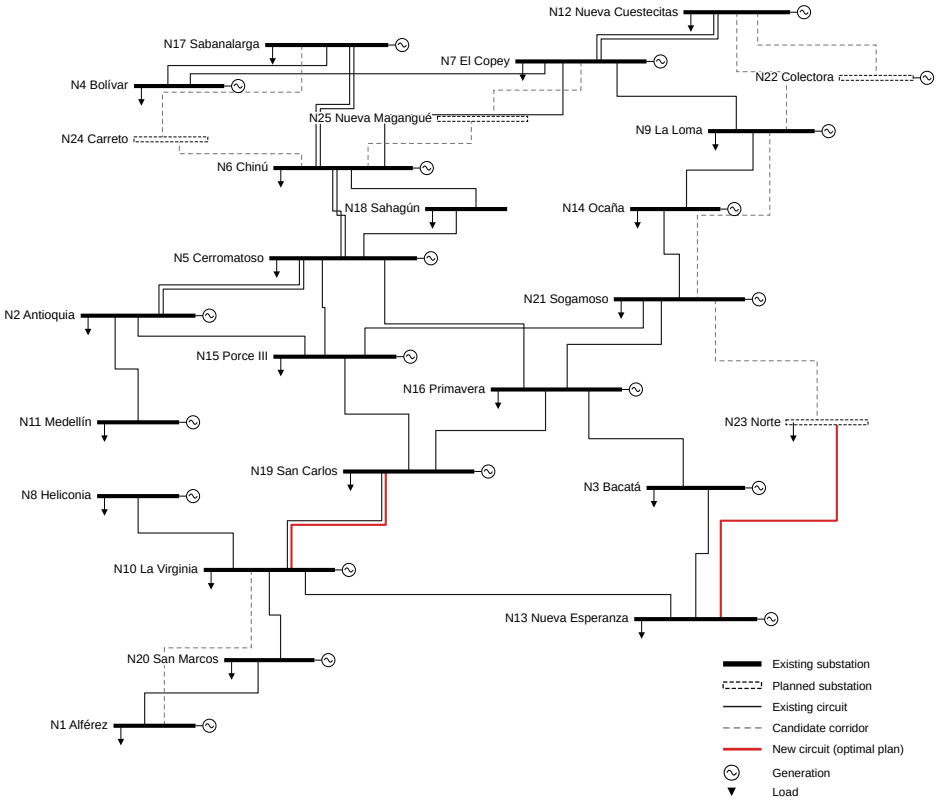


Figure A12. Optimal expansion plan of the 500 kV backbone under the BTMI allocation, $\bar{\alpha} = 15\%$, USD 85.0M. Existing circuits in black, candidate corridors not built in gray dashed lines and new circuits, including reinforcements of existing corridors, in red.

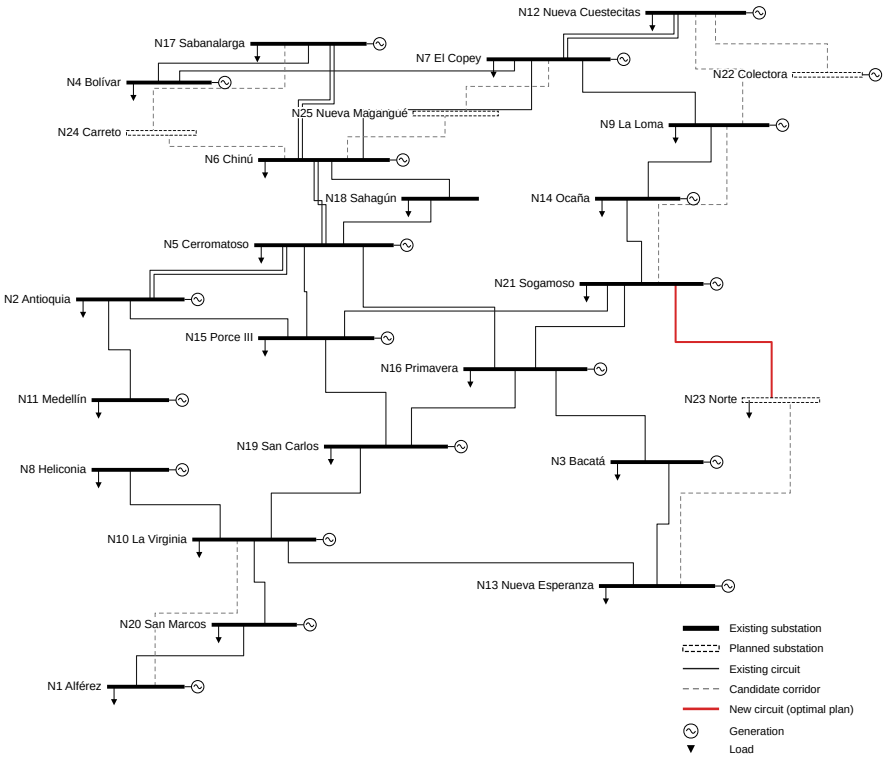


Figure A13. Optimal expansion plan of the 500 kV backbone under the BTMI allocation, $\bar{\alpha} = 20\%$, USD 73.0M. Existing circuits in black, candidate corridors not built in gray dashed lines and new circuits, including reinforcements of existing corridors, in red.

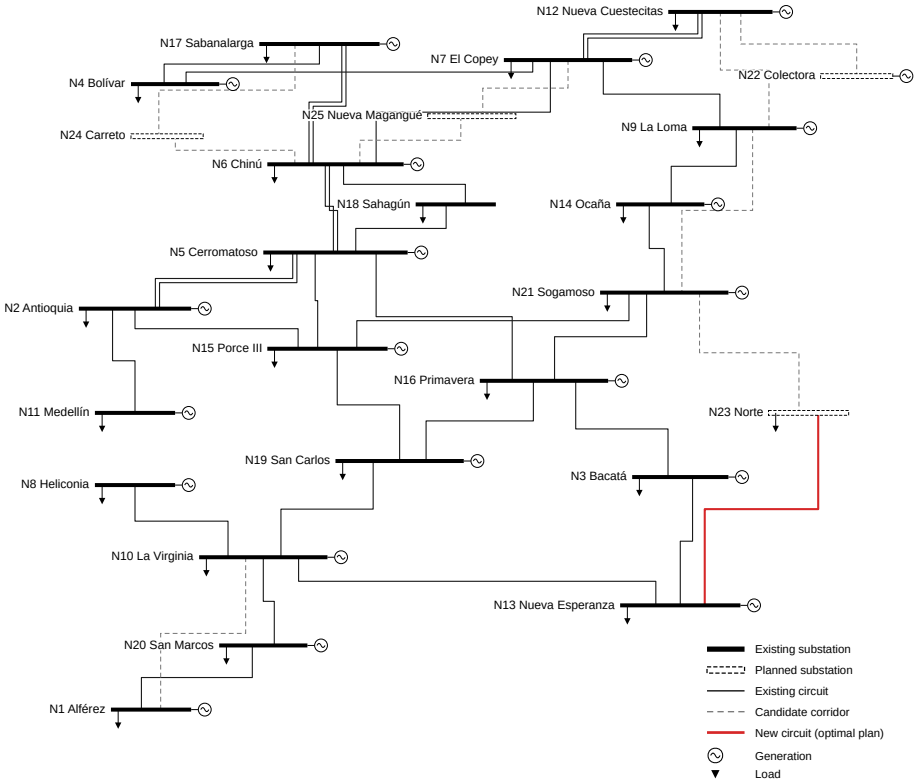


Figure A14. Optimal expansion plan of the 500 kV backbone under the BTMI allocation, $\bar{\alpha} = 25\%$, USD 24.7M. Existing circuits in black, candidate corridors not built in gray dashed lines and new circuits, including reinforcements of existing corridors, in red.

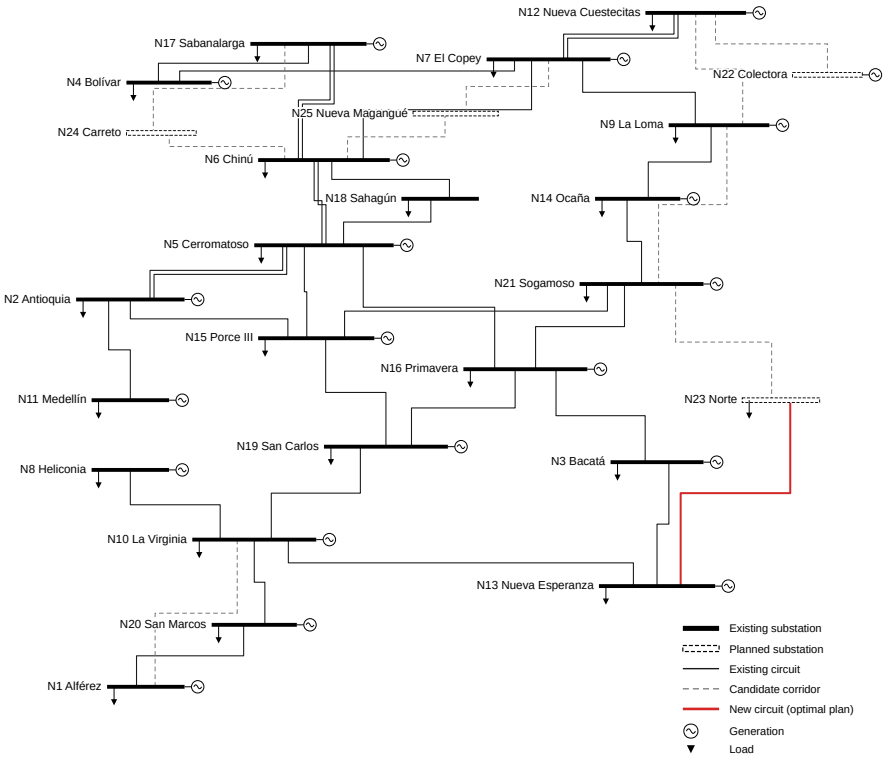


Figure A15. Optimal expansion plan of the 500 kV backbone under the BTMI allocation, $\bar{\alpha} = 30\%$, USD 24.7M. Existing circuits in black, candidate corridors not built in gray dashed lines and new circuits, including reinforcements of existing corridors, in red.

References

1. Garver, L.L. Transmission network estimation using linear programming. *IEEE Trans. Power Appar. Syst.* **1970**, *PAS-89*, 1688–1697. [CrossRef]
2. Villasana, R.; Garver, L.L.; Salon, S.J. Transmission network planning using linear programming. *IEEE Trans. Power Appar. Syst.* **1985**, *PAS-104*, 349–356. [CrossRef]
3. OMIE—Operador del Mercado Ibérico de Energía. Electricity Market Data: Centralized Generation and Behind-The-Meter Self-Consumption in Spain, 2018–2025. 2025. Available online: https://www.omie.es/en/ (accessed on 14 November 2026).
4. Clean Energy Council. *Clean Energy Australia Report 2026*; Technical Report; Clean Energy Council: Melbourne, Australia, 2026.
5. California Energy Commission. 2025 Total System Electric Generation. Includes the 2025 IEPR Estimates of Gross Consumption, Net Energy for Load and Behind-The-Meter PV Generation. 2026. Available online: https://www.energy.ca.gov/data-reports/energy-almanac/california-electricity-data/2025-total-system-electric-generation (accessed on 14 November 2026).
6. Empresa de Pesquisa Energética (EPE). *National Energy Balance 2026: Summary Report, Base Year 2025*; Technical Report; EPE: Rio de Janeiro, Brazil, 2026. (In Portuguese)
7. Fraunhofer Institute for Solar Energy Systems ISE. Öffentliche Nettostromerzeugung in Deutschland 2025. 2026. Available online: https://www.ise.fraunhofer.de/content/dam/ise/de/documents/presseinformationen/2026/0126_ISE_d_PI_Jahreszahlen%202025.pdf (accessed on 14 November 2026).
8. Gestore dei Servizi Energetici (GSE). *Solar Photovoltaics: Statistical Report 2024*; Technical Report; GSE: Rome, Italy, 2025. (In Italian)
9. Enerdata. Renewable Sources Covered a Record 41% of Italy's Power Demand in 2024. 2025. Available online: https://www.enerdata.net/publications/daily-energy-news/renewable-sources-covered-record-41-italys-power-demand-2024.html (accessed on 14 November 2026).
10. Entidade Reguladora dos Serviços Energéticos (ERSE). *Report on Self-Consumption*; Technical Report; ERSE: Lisbon, Portugal, 2025. (In Portuguese)
11. Mining and Energy Planning Unit (UPME). *Electricity Demand Projections 2026–2040*; Technical Report; UPME: Bogotá, Colombia, 2026. (In Spanish)
12. SER Colombia. *Renewables Report 2025*; Technical Report; Asociación de Energías Renovables SER Colombia: Bogotá, Colombia, 2025. (In Spanish)
13. Australian Energy Market Operator (AEMO). *2026 Integrated System Plan for the National Electricity Market*; Technical Report; AEMO: Melbourne, Australia, 2026.
14. California Independent System Operator (CAISO). *2025–2026 Transmission Plan*; Technical Report; CAISO: Folsom, CA, USA, 2026.
15. Ministry of Mines and Energy (MME) and Energy Research Office (EPE) of Brazil. *Ten-Year Energy Expansion Plan 2035*; Technical Report; MME/EPE: Brasília, Brazil, 2026. (In Portuguese)
16. Ministry for the Ecological Transition and the Demographic Challenge (MITECO). *Development Plan for the Electricity Transmission Grid, 2021–2026*; Technical Report; Government of Spain: Madrid, Spain, 2022. Approved by the Council of Ministers on 22 March 2022; Planning Horizon 2026. Original Spanish Title: *Plan de Desarrollo de la Red de Transporte de Energía Eléctrica 2021–2026*. Available online : https://www.fao.org/faolex/en/documents/LEX-FAOC207904/plan-nacional-integrado-de-energia-y-clima-pniec-2021-2030-esp-2020 (accessed on 14 November 2026).
17. Ministry for the Ecological Transition and the Demographic Challenge (MITECO). Joan Groizard Presents the Results of the New Electricity Planning Proposal with a 2030 Horizon. 2026. Available online: https://www.miteco.gob.es/es/prensa/ultimas-noticias/2026/septiembre/joan-groizard-avanza-el-resultado-de-la-nueva-propuesta-de-plani.aspx (accessed on 14 November 2026). (In Spanish)
18. 50Hertz; Amprion; TenneT; TransnetBW. *Grid Development Plan for Electricity 2037/2045, Version 2025, Second Draft*; Technical Report; German Transmission System Operators: Berlin, Germany, 2026. (In German)
19. Terna. *Development Plan 2025 of the National Transmission Grid*; Technical Report; Terna S.p.A.: Rome, Italy, 2025. (In Italian)
20. Redes Energéticas Nacionais (REN). *Development and Investment Plan of the Electricity Transmission Network 2025–2034 (PDIRT-E 2024)*; Technical Report; REN: Lisbon, Portugal, 2025. (In Portuguese)
21. Mining and Energy Planning Unit (UPME). *Transmission Expansion Plan 2025–2039*; Technical Report; UPME: Bogotá, Colombia, 2025. (In Spanish)
22. California Independent System Operator (CAISO). *2025–2026 Transmission Planning Process: Unified Planning Assumptions and Study Plan*; Technical Report; CAISO: Folsom, CA, USA, 2025.
23. California Independent System Operator (CAISO). 2026–2027 Transmission Planning Process: Stakeholder Meeting. Presentation, 24 February 2026. 2026. Available online: https://stakeholdercenter.caiso.com/InitiativeDocuments/Presentation-2026-2027-Transmission-Planning-Process-Feb-24-2026.pdf (accessed on 14 November 2026).

24. Government of Spain. Order TEC/212/2019 of 25 February, Initiating the Procedure for Proposals for the Development of the Electricity Transmission Grid with a 2026 Horizon. Official State Gazette (Boletín Oficial del Estado), No. 52, 1 March 2019. 2019. Available online: https://www.boe.es/diario_boe/txt.php?id=BOE-A-2019-2965 (accessed on 14 November 2026).
25. Garcés, L.P.; Conejo, A.J.; García-Bertrand, R.; Romero, R. A bilevel approach to transmission expansion planning within a market environment. *IEEE Trans. Power Syst.* **2009**, *24*, 1513–1522. [CrossRef]
26. González Cabrera, N.; Fuerte Ledezma, L.F.; Gutiérrez Alcaraz, G. Transmission Expansion Planning with Network Reinforcement Based on Reliability Assessment. *Sci. Tech.* **2015**, *20*, 162–171. (In Spanish) [CrossRef]
27. Vargas-Robayo, C.Y.; Blanco-Valbuena, D.F.; Montoya-Giraldo, O.D.; Giral-Ramírez, D.A. Evaluation of Linear and Nonlinear Programming Models for Transmission System Planning in the GAMS Software. *Tecnura* **2021**, *25*, 16–50. (In Spanish) [CrossRef]
28. Kim, W.W.; Park, J.K.; Yoon, Y.T.; Kim, M.K. Transmission expansion planning under uncertainty for investment options with various lead-times. *Energies* **2018**, *11*, 2429. [CrossRef]
29. Giannelos, S.; Jain, A.; Borozan, S.; Falugi, P.; Moreira, A.; Bhakar, R.; Mathur, J.; Strbac, G. Long-term expansion planning of the transmission network in India under multi-dimensional uncertainty. *Energies* **2021**, *14*, 7813. [CrossRef]
30. Khastieva, D.; Hesamzadeh, M.R.; Vogelsang, I.; Rosellón, J.; Amelin, M. Value of energy storage for transmission investments. *Energy Strategy Rev.* **2019**, *24*, 94–110. [CrossRef]
31. Barrera-Singaña, C.; Comech, M.P.; Arcos, H. A comprehensive review on the integration of renewable energy through advanced planning and optimization techniques. *Energies* **2025**, *18*, 2961. [CrossRef]
32. Lee, S.; Peschon, J.; Germond, A. *Impact on Transmission Requirements of Dispersed Storage and Generation*; Technical Report EPRI EM-1192; Electric Power Research Institute (EPRI): Palo Alto, CA, USA, 1979.
33. Shugar, D. Photovoltaics in the utility distribution system: The evaluation of system and distributed benefits. In Proceedings of the IEEE Conference on Photovoltaic Specialists, Kissimmee, FL, USA, 21–25 May 1990; Volume 2, pp. 836–843. [CrossRef]
34. Li, X.; Zielke, G.K. One-year deferral method for estimating avoided transmission and distribution costs. *IEEE Trans. Power Syst.* **2005**, *20*, 1408–1414. [CrossRef]
35. De Oliveira-De Jesus, P.M.; Ponce de Leão, M.T.; Yusta, J.M.; Khodr, H.M. A General Framework for the Remuneration of Costs and Benefits of Distributed Generation. In Proceedings of the 2006 IEEE/PES Transmission & Distribution Conference and Exposition: Latin America, Caracas, Venezuela, 15–18 August 2006; pp. 1–6. [CrossRef]
36. De Oliveira-De Jesus, P.M. Remuneration of Distributed Generation: A Holistic Approach. Ph.D. Thesis, Faculdade de Engenharia da Universidade do Porto, Porto, Portugal, 2007.
37. Mendez, V.H.; Rivier, J.; de la Fuente, J.I.; Gomez, T.; Arceluz, J.; Marin, J.; Madurga, A. A Monte Carlo approach for assessment of investments deferral in radial distribution networks with distributed generation. In Proceedings of the 2003 IEEE Bologna Power Tech Conference, Bologna, Italy, 23–26 June 2003; Volume 1, pp. 1–8. [CrossRef]
38. Luo, F.; Zhao, J.; Qiu, J.; Foster, J.; Peng, Y.; Dong, Z. Assessing the transmission expansion cost with distributed generation: An Australian case study. *IEEE Trans. Smart Grid* **2014**, *5*, 1892–1904. [CrossRef]
39. Muhs, J.; Palomino, A.; Moyer, K. Distributed Generation Resources and Their Impacts on Long-Term Transmission Need. Energy Systems Integration Group (ESIG). 2024. Available online: https://www.esig.energy/distributed-generation-resources-and-their-impacts-on-long-term-transmission-need/ (accessed on 14 November 2026).
40. Laws, N.D.; Webber, M.E.; Chen, D. Valuing distributed energy resources for non-wires alternatives. *Electr. Power Syst. Res.* **2024**, *234*, 110521. [CrossRef]
41. Keen, J.; Giraldez, J.; Cook, E.; Eiden, A.; Placide, S.; Hirayama, A.; Monson, B.; Mino, D.; Eldali, F. *Distribution Capacity Expansion: Current Practice, Opportunities and Decision Support*; Technical Report NREL/TP-6A40-83892; National Renewable Energy Laboratory: Golden, CO, USA, 2022.
42. Carvallo, J.P.; Bieler, S.; Collins, M.T.; Mueller, J.; Gehbauer, C.; Gotham, D.J.; Larsen, P.H. A framework to measure the technical, economic, and rate impacts of distributed solar, electric vehicles, and storage. *Appl. Energy* **2021**, *297*, 117160. [CrossRef]
43. Pudaruth, G.R.; Li, F. Capacity credit evaluation: A literature review. In Proceedings of the Third International Conference on Electric Utility Deregulation and Restructuring and Power Technologies (DRPT), Nanjing, China, 6–9 April 2008. [CrossRef]
44. Liu, G.; Vrakopoulou, M.; Mancarella, P. Assessment of the Capacity Credit of Renewables and Storage in Multi-Area Power Systems. *IEEE Trans. Power Syst.* **2021**, *36*, 2334–2344. [CrossRef]
45. De Oliveira-De Jesus, P.M.; Yusta, J.M. Model for optimal sizing of photovoltaic and battery energy storage systems considering an efficient scheme for contracted power capacity. *J. Energy Storage* **2026**, *180*, 124014. [CrossRef]
46. De Oliveira-De Jesus, P.M.; Yusta, J.M. Optimal power dispatch for maximum energy community welfare by considering closed distribution systems and renewable sources. *Energies* **2024**, *17*, 4707. [CrossRef]
47. Bandeiras, F.; Gomes, Á.; Gomes, M.; Coelho, P. Application and challenges of coalitional game theory in power systems for sustainable energy trading communities. *Energies* **2023**, *16*, 8115. [CrossRef]

48. Rangelova, K.; Jones, D. Solar Electricity Every Hour of Every Day is Here and It Changes Everything. Report, Ember. 2025. Available online: https://ember-energy.org/app/uploads/2025/06/Ember-24-Hour-Solar-Electricity-June-2025-6.pdf (accessed on 14 November 2026).
49. Red Eléctrica de España. Day-Ahead Market. Spanish Electricity System Report 2024, Red Eléctrica de España. 2025. Available online: https://www.sistemaelectrico-ree.es/en/2024/spanish-electricity-system/markets/day-ahead-market (accessed on 14 November 2026).
50. Consolinno Energy. Solar Peak Act 2025 (Solarspitzengesetz): What Is Now Changing for Photovoltaic Owners. 2025. Available online: https://consolinno.de/en/solarspitzengesetz-2025-was-sich-jetzt-fuer-photovoltaik-besitzer-aendert/ (accessed on 14 November 2026).
51. Lawrence Berkeley National Laboratory. *Early Market Impacts of the California Net Billing Tariff (NEM 3.0): Technical Brief*; Technical Report; LBNL: Berkeley, CA, USA, 2024.
52. Lu, Q.; Liu, M. A multi-criteria compromise ranking decision-making approach for analysis and evaluation of community-integrated energy service system. *Energy* **2024**, *306*, 132439. [CrossRef]
53. Petrichenko, L.; Mutule, A.; Hlusovs, S.; Zarins, R.; Novosads, P.; Diahovchenko, I. Multi-Criteria Decision Analysis Framework for Evaluating Tools Supporting Renewable Energy Communities. *Sustainability* **2026**, *18*, 29. [CrossRef]
54. Mining and Energy Planning Unit (UPME). *Reference Generation–Transmission Expansion Plan 2022–2036*; Technical Report; UPME: Bogotá, Colombia, 2023. (In Spanish)
55. Energy and Gas Regulation Commission (CREG). *Resolution CREG 030 of 2018: Regulation of Small-Scale Self-Generation and Distributed Generation in the National Interconnected System*; Technical Report; CREG: Bogotá, Colombia, 2018.
56. Energy and Gas Regulation Commission (CREG). *Resolution CREG 174 of 2021: Regulation of Small-Scale Self-Generation and Distributed Generation in the National Interconnected System*; Technical Report; CREG: Bogotá, Colombia, 2021. (In Spanish)
57. Congress of the Republic of Colombia. *Law 2099 of 2021: Provisions for the Energy Transition, the Dynamization of the Energy Market and the Economic Reactivation of the Country*; Technical Report; Congreso de la República: Bogotá, Colombia, 2021. (In Spanish)
58. Presidency of the Republic of Colombia. *Decree 2236 of 2023: Partial Regulation of Article 235 of Law 2294 of 2023 on Energy Communities*; Technical Report; Presidencia de la República: Bogotá, Colombia, 2023. (In Spanish)
59. Ministry of Mines and Energy of Colombia. *Resolution 40509 of 2024: Regulation of the Registry of Energy Communities and Criteria for Targeting and Prioritizing Public Resources for Energy Communities*; Technical Report; Ministerio de Minas y Energía: Bogotá, Colombia, 2024. (In Spanish)
60. Energy and Gas Regulation Commission (CREG). *Resolution CREG 101 072 of 2025: Harmonization of the Regulation for the Integration of Energy Communities into the National Energy System*; Technical Report; CREG: Bogotá, Colombia, 2025. (In Spanish)
61. XM S.A. E.S.P. PARATEC: Technical Parameters of the National Interconnected System. 2026. Available online: https://paratec.xm.com.co (accessed on 15 October 2026). (In Spanish)
62. Energy and Gas Regulation Commission (CREG). *Resolution CREG 011 of 2009: Methodology and Tariff Formulas for the Remuneration of Electricity Transmission in the National Transmission System*; Technical Report; CREG: Bogotá, Colombia, 2009. (In Spanish)
63. Institute of Hydrology, Meteorology and Environmental Studies (IDEAM) and Mining and Energy Planning Unit (UPME). *Atlas of Solar Radiation, Ultraviolet Radiation and Ozone of Colombia*; Technical Report; IDEAM and UPME: Bogotá, Colombia, 2018. (In Spanish)
64. Hart, W.E.; Watson, J.P.; Woodruff, D.L. Pyomo: Modeling and solving mathematical programs in Python. *Math. Program. Comput.* **2011**, *3*, 219–260. [CrossRef]
65. Gurobi Optimization, LLC. Gurobi Optimizer Reference Manual. 2026. Available online: https://docs.gurobi.com/projects/optimizer/en/14.0/index.html (accessed on 15 October 2026).

Disclaimer/Publisher's Note: The statements, opinions and data contained in all publications are solely those of the individual author(s) and contributor(s) and not of MDPI and/or the editor(s). MDPI and/or the editor(s) disclaim responsibility for any injury to people or property resulting from any ideas, methods, instructions or products referred to in the content.